Chapter II
Background notions and state of the art

Content

Summary

It is assumed that the reader is familiar with the classical notions of Solid Mechanics, Plasticity and Finite elements. These notions will not be recalled here.

This chapter briefly introduces some of the less classical notions that will be used throughout this thesis.

The most important are:

- the notions of Delaunay tessellation, Voronoi cells and natural neighbours that constitute the basic tools of the Natural Neighbours Method, also called the Natural Elements Method (NEM);

- the classical approach of the NEM based on the virtual work principle;

- the Fraeijs de Veubeke functional and variational principle.

We do not intend to cover these subjects in a very detailed manner.

The purpose is to provide the reader with some basic information in a simple didactic way and to examine the state of the art on these aspects.

For more information, a fairly complete presentation of the NEM is available in a recent monography [CHINESTA et al.,2009].

On the other hand, although Linear Elastic Fracture Mechanics (LEFM) is a basic science that can be considered as a part of Solid Mechanics, since chapters V and VI of this thesis propose new approaches for problems of LEFM, some of the basic ingredients of this science are also briefly recalled.

II.1. The tools of the Natural Neighbours Method (NEM)

II.1.1. Delaunay tessellation, Voronoi cells and natural neighbours

II.1.1.1. Delaunay tessellation

Consider a 2D domain containing a set of nodes, some of which can be located on the domain contour.

A Delaunay triangle is a triangle the corners of which are 3 nodes of the set and has the property that its circumcircle does not contain any other node than the 3 nodes defining its 3 corners.

The Delaunay tessellation of the domain is the set of the Delaunay triangles constructed with the nodes of the domain.

There are many methods to construct the Delaunay tessellation on a given set of nodes.

An excellent review of these methods is given in [SHEWCHUK J. R. (1996)].

Free software for the construction of a Delaunay tessellation is available on Internet.

As an example, figure II.1 shows a domain with a set of nodes and figure II.2 gives the corresponding Delaunay tessellation.

Figure II.1.

Domain contour and nodes

In this example, the interior nodes are randomly distributed.

There are 10 nodes on the contour and 15 nodes inside.

Figure II.2.

Delaunay tessellation constructed on the domain of figure II.1

There are 38 Delaunay triangles.
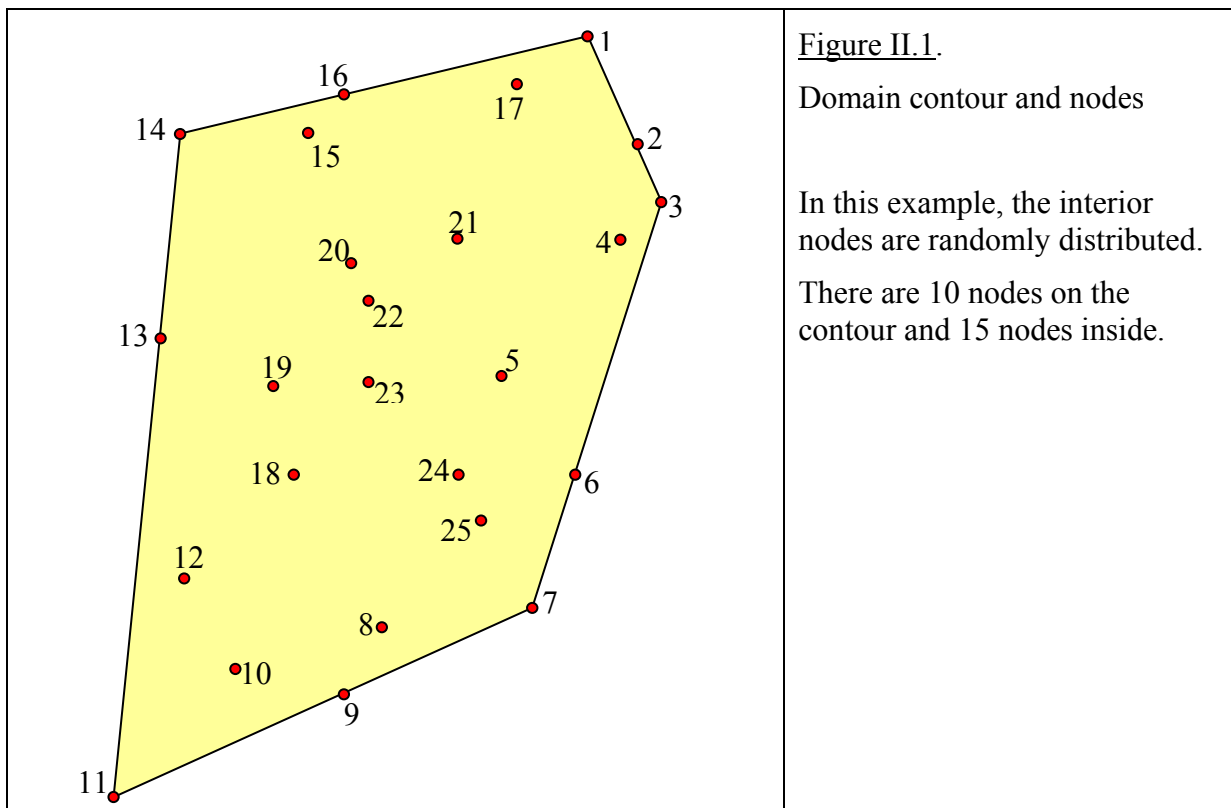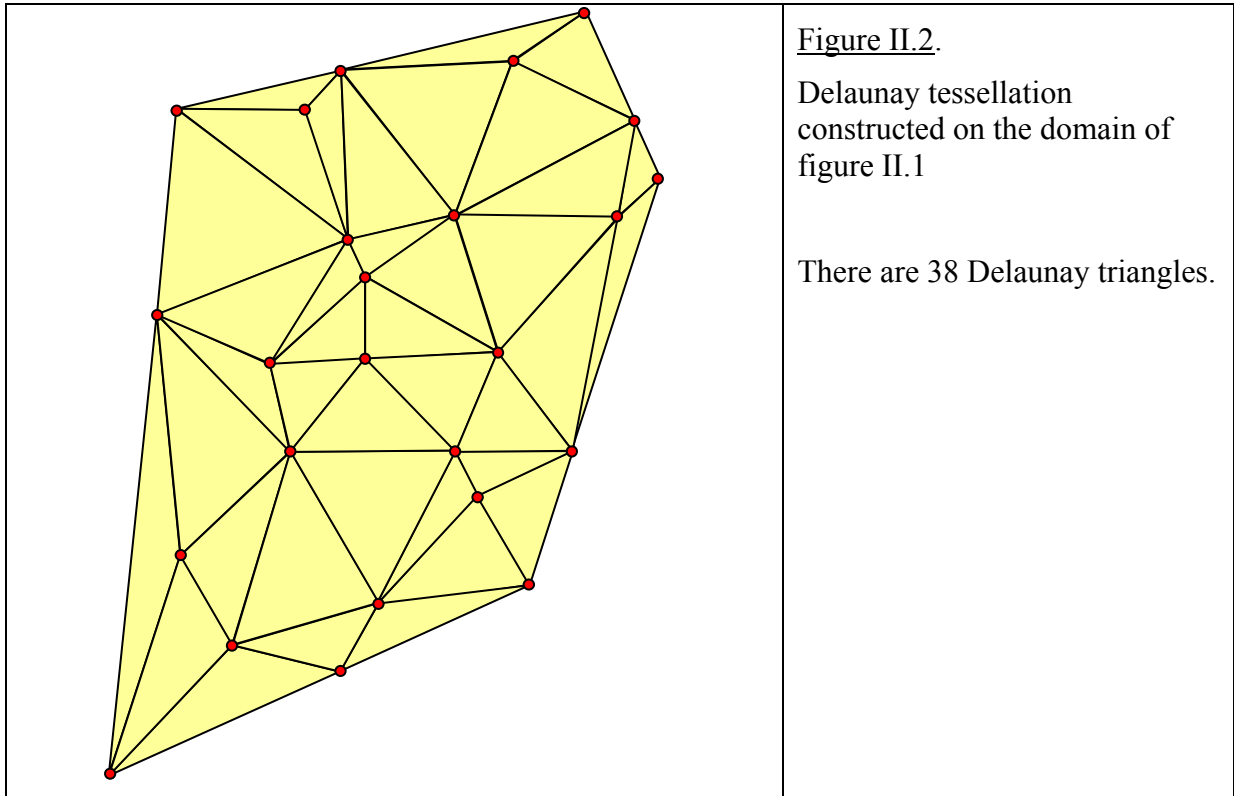
II.1.1.2. Voronoi polygons, Voronoi cells and natural neighbours

a. Case of a convex domain

For simplicity, consider the case of figure II.2.

The edges of the Voronoi polygon associated with a node I are simply the segments joining the successive centers of the circumcircles of the Delaunay triangles sharing node I.

The Voronoi cells are the parts of the Voronoi polygons inside the domain contour.

TheVoronoi cell associated with a given node I has the following property:

for any point $X = (X_1, X_2)$ inside this cell, we have:

$$d(X, I) < d(X, J) \ \forall J \neq I \tag{II.1}$$

where $d(A, B)$ is the distance between 2 points A and B.

Figure II.3 shows the Voronoi polygons associated with the nodes of the domain of figure II.1.

Figure II.4 shows the corresponding Voronoi cells.

A Voronoi cell having at least 1 edge belonging to the domain contour is called an exterior Voronoi cell.
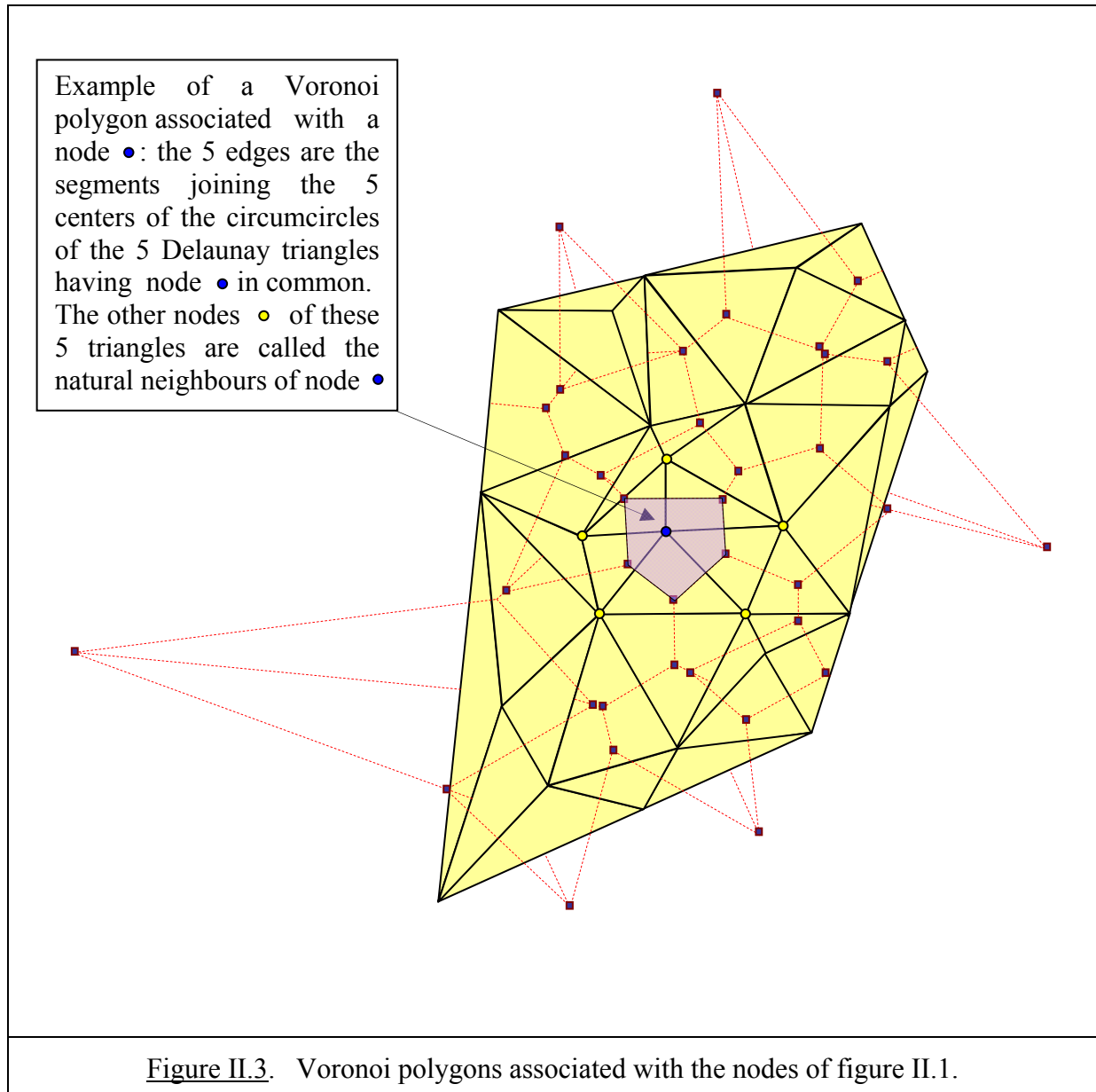
A Voronoi cell no edge of which belongs to the domain contour is called an interior Voronoi cell. The corresponding node is inside the domain.

Figure II.5 shows this classification for the treated example.

Figure II.3 also introduces the notion of natural neighbours.

The *k* corners of the Voronoi polygon associated with a node *I* are the centers of the circumcircles of *k* Delaunay triangles sharing node *I*.

The *k* other nodes of these triangles are defined as the natural neighbours of node *I* because no other node of the domain is closer to node *I*.

Example of a Voronoi polygon associated with a node ●: the 5 edges are the segments joining the 5 centers of the circumcircles of the 5 Delaunay triangles having node ● in common. The other nodes ○ of these 5 triangles are called the natural neighbours of node ●

Figure II.3. Voronoi polygons associated with the nodes of figure II.1.

The Voronoi polygon associated with this node is a triangle. The Voronoi cell associated with the same node is the shaded quadrilateral, i.e. the part of the triangle inside the domain contour.

Figure II.4. Voronoi cells associated with the nodes of figure II.1.

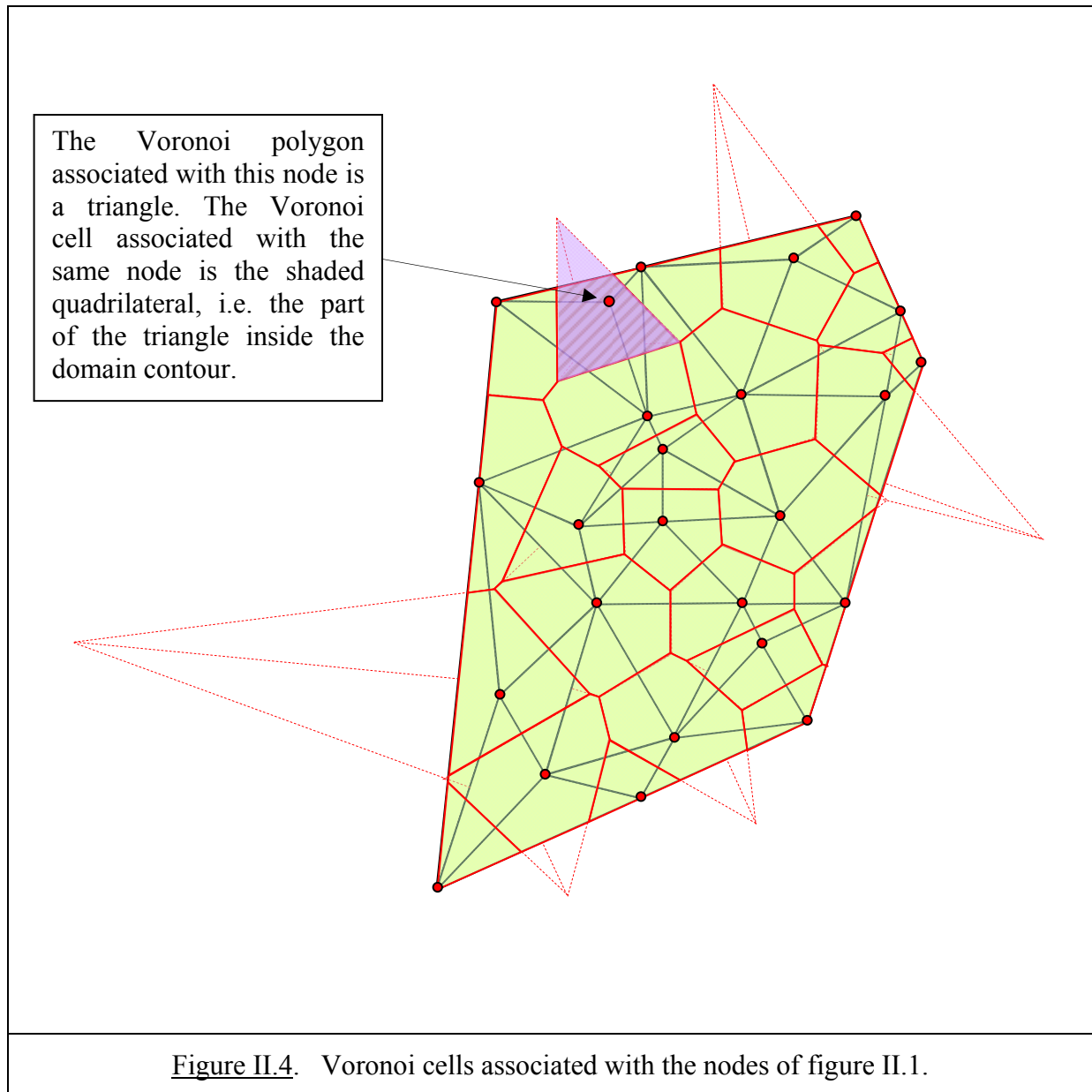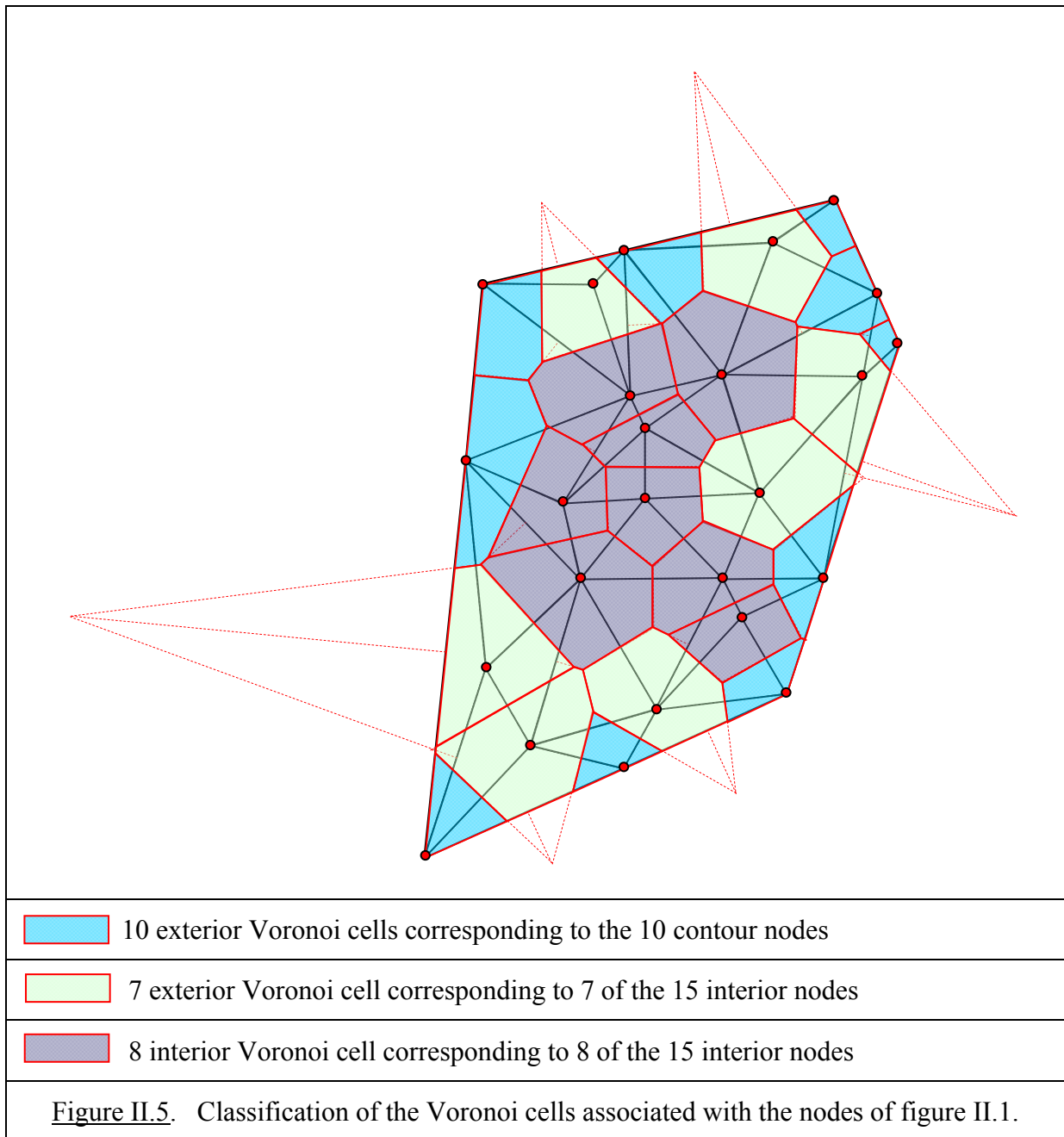|	
🟦	10 exterior Voronoi cells corresponding to the 10 contour nodes
⬜	7 exterior Voronoi cell corresponding to 7 of the 15 interior nodes
🟪	8 interior Voronoi cell corresponding to 8 of the 15 interior nodes

Figure II.5.   Classification of the Voronoi cells associated with the nodes of figure II.1.

b. Case of a non convex domain

Let us consider the example of figure II.6
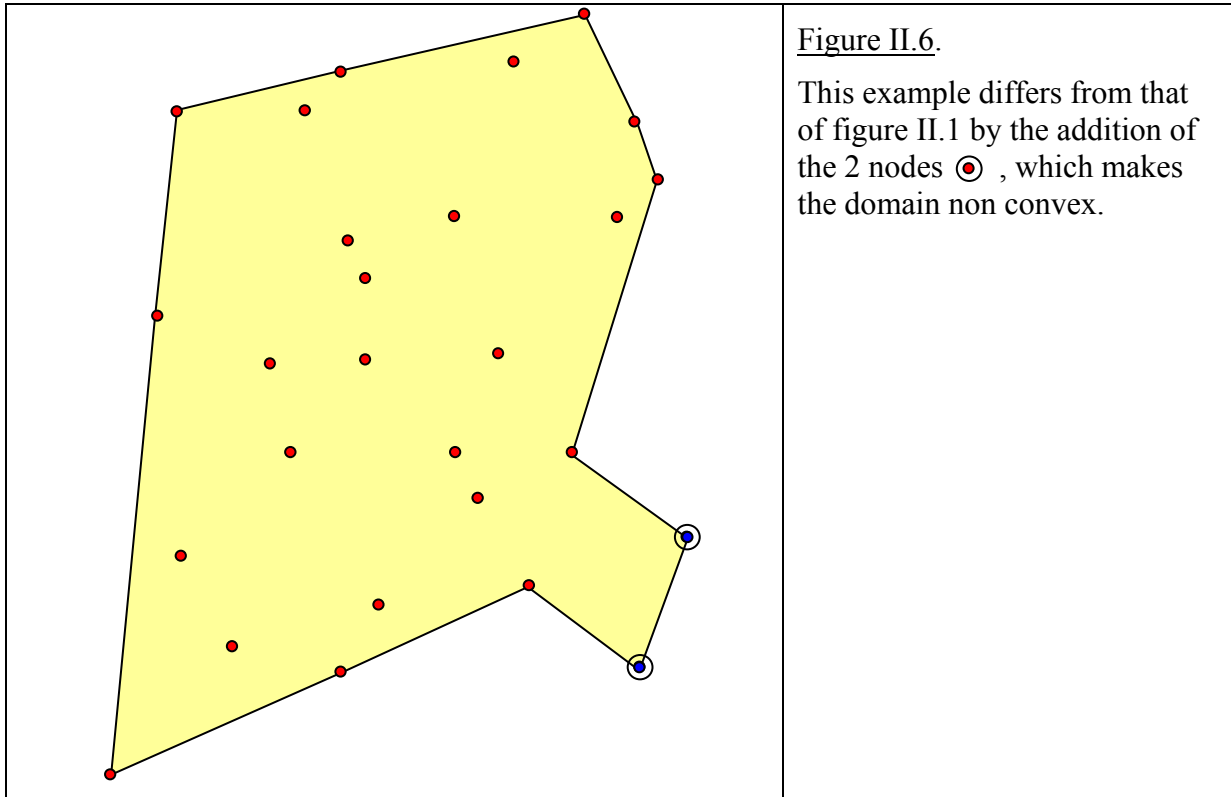

Figure II.6.

This example differs from that of figure II.1 by the addition of the 2 nodes ⊙ , which makes the domain non convex.

For the case of non convex domains (or discontinuous domains or multi-connected domains), the definition of a Voronoi cell is extended as follows:

TheVoronoi cell associated with a given node I has the following property:

for any point $X = (X_1, X_2)$ inside this cell, we have:

$$d(X,I) < d(X,J) \ \forall J \neq I \,, \ S_{X \to I} \cap S = 0 \ \ , \ S_{X \to J} \cap S = 0 \qquad \text{(II.2)}$$

where $S_{A \to B}$ means the segment going from A to B and S is the contour of the domain.

Note that for discontinuous or multi-connected domains, there are several domain contours $S_i \,, \ i=1,m$ but we continue using the symbol S to denote the set of all these contours:

$$S = S_1 \cup S_2 \cup ..... \cup S_m$$

For the example treated, figure II.7 shows the Delaunay triangulation obtained.

Note that the circumcircle of triangle "*ni-nj-nk*" includes node "*s*", which is valid because of the properties of the Voronoi cells in the case of a non convex domain.

The Voronoi cells for the example treated are shown on figure II.8.
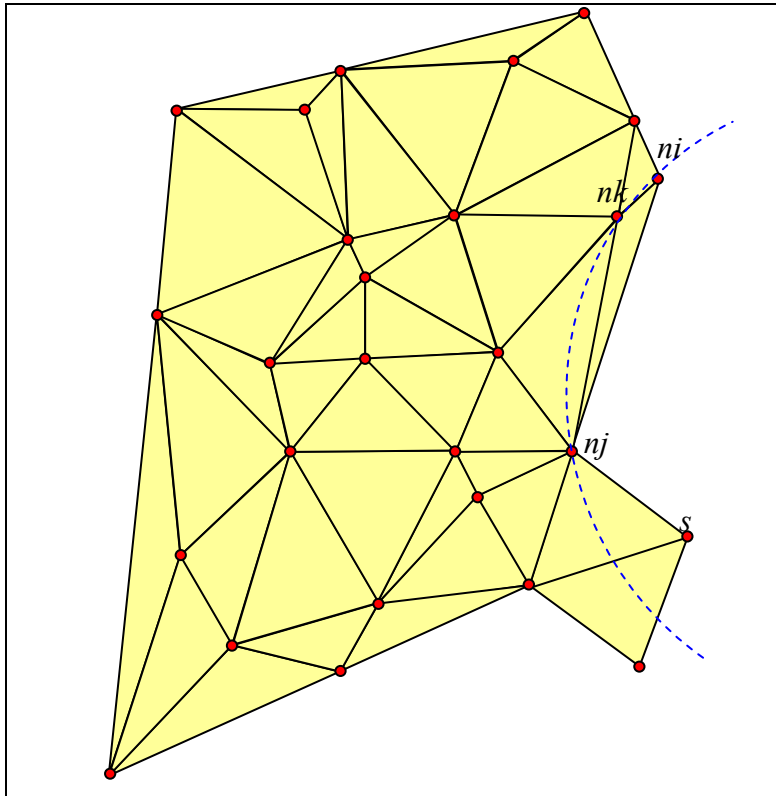
Figure II.7.

The Delaunay tessellation of the non convex domain.
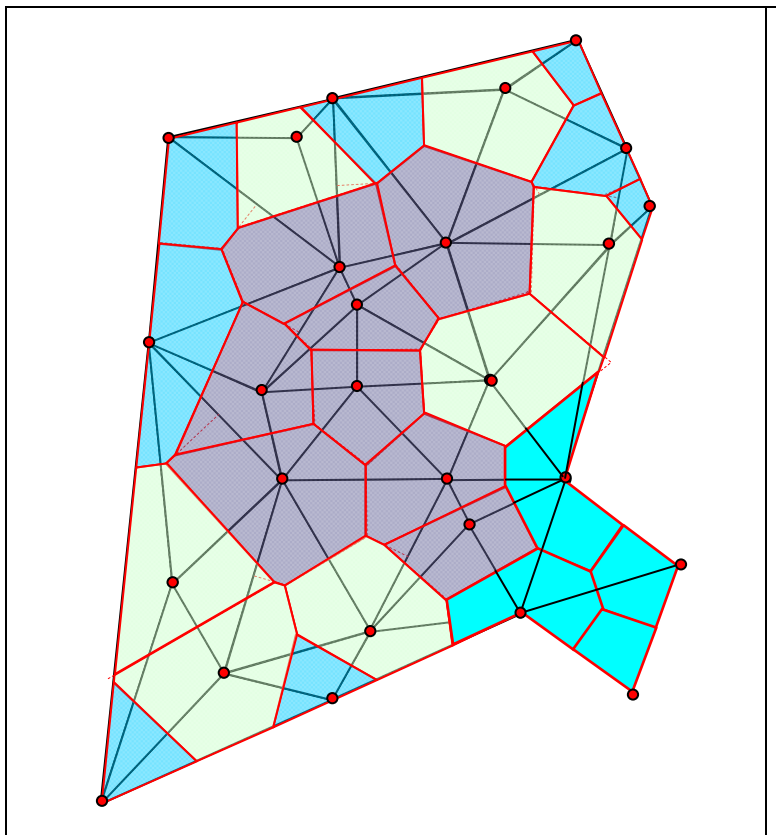
There are 40 Delaunay triangles.

Figure II.8.

The Voronoi cells of the non convex domain

12 exterior Voronoi cells corresponding to the 12 contour nodes

7 exterior Voronoi cells corresponding to 7 of the 15 interior nodes

8 interior Voronoi cells corresponding to 8 of the 15 interior nodes

II.1.1.3. Uniqueness

For a given domain and a given set of nodes, the Delaunay tessellation may be not unique.

As an example, for the rectangular domain with 4 nodes of figure II.9, we have 2 possible Delaunay tessellations as shown in figure II.10.

However, for a given domain and a given set of nodes, the set of Voronoi cells is unique.

For the present example, it is illustrated on figure II.11.

Figure II.9.

Rectangular domain with 4 nodes

Figure II.10.a.

Rectangular domain with 4 nodes.

First solution for the Delaunay tessellation.

Figure II.10.b.

Rectangular domain with 4 nodes.

Second solution for the Delaunay tessellation.

Figure II.11.

Rectangular domain with 4 nodes.

Unique solution for the set of Voronoi cells.
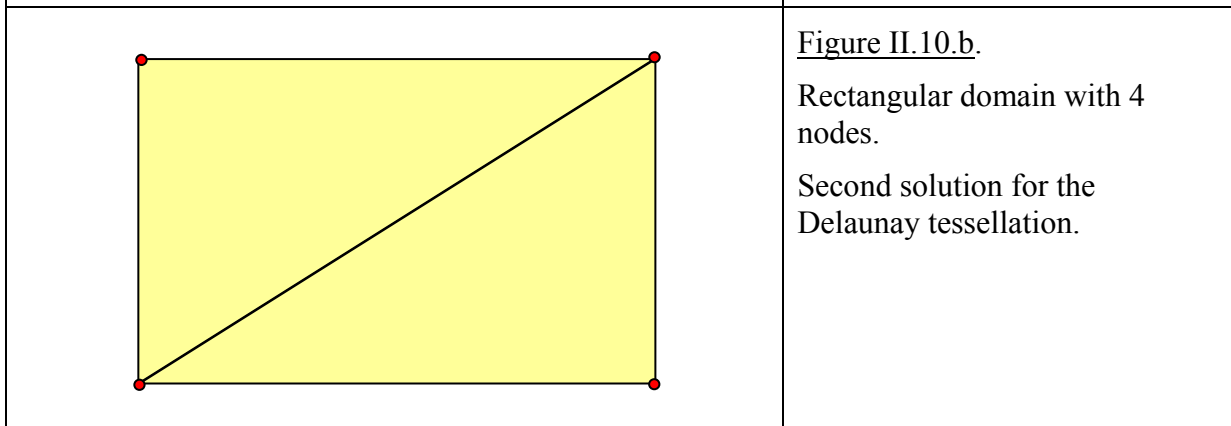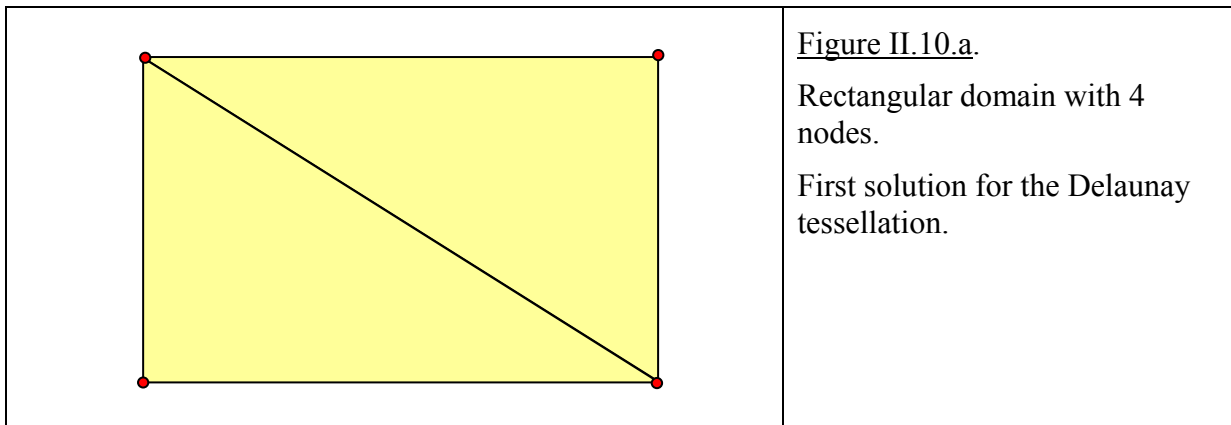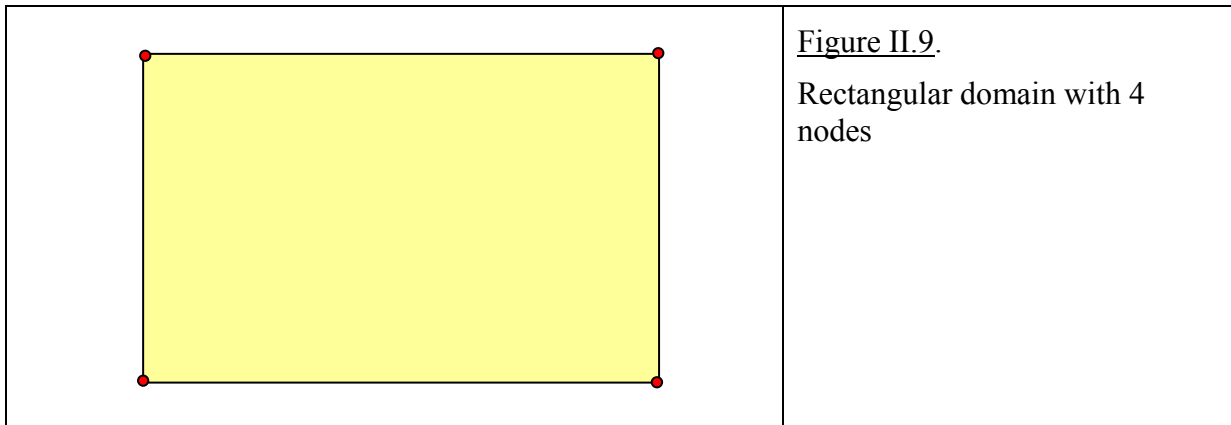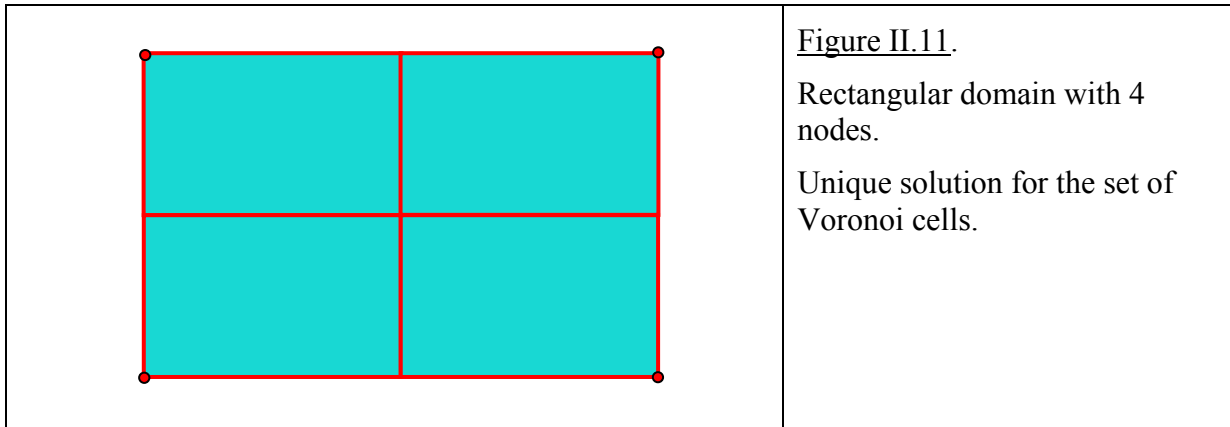
II.1.2. Laplace interpolation

II.1.2.1. Definition

Let u_i^J be the displacement components of node J.

As usual, the displacement field in the domain can be interpolated by

$$u_i = \sum_{J=1}^{N} \Phi_J u_i^J \tag{II.3}$$

where Φ_J is an interpolation function associated with node J.

It can be defined in many different ways.

In the finite element method, the various choices for Φ_J use both the notion of nodes and the notion of sub-domains (the finite elements).

In this thesis, we use the Laplace interpolation function [BELIKOV V. V. et al. (1997), HIYOSHI H. and SUGIHARA K. (1999)] that only uses the notion of nodes. For the calculation of this function, the Voronoi cells are used and it could be argued that these cells constitute a division of the domain into sub-domains. However, these cells are uniquely defined by the nodes, which is not the case with finite elements.

II.1.2.2. Laplace interpolation function for a point X inside the domain

The Laplace interpolation function $\Phi_J(X)$ associated with a node J is positive if point X is close to node J and is equal to 0 if point X is far enough from J.

More precisely, the domain on which $\Phi_J(X) > 0$ is explained on figure II.12.

It consists of the union of the circumcircles of the Delaunay triangles sharing node J.

To calculate the Laplace interpolation functions Φ_J, we use the Bowyer-Watson algorithm [BOWYER A.(1981), WATSON D.F. (1981)].

It consists of the 4 steps described below and illustrated by figures II.13a to d.

Node J

Domain on which the Laplace function Φ_J is non zero

If $X(X_1, X_2)$ is inside this domain, $\Phi_J(X) > 0$

else, $\Phi_J(X) = 0$

Figure II.12. Definition domain of the Laplace interpolation function.
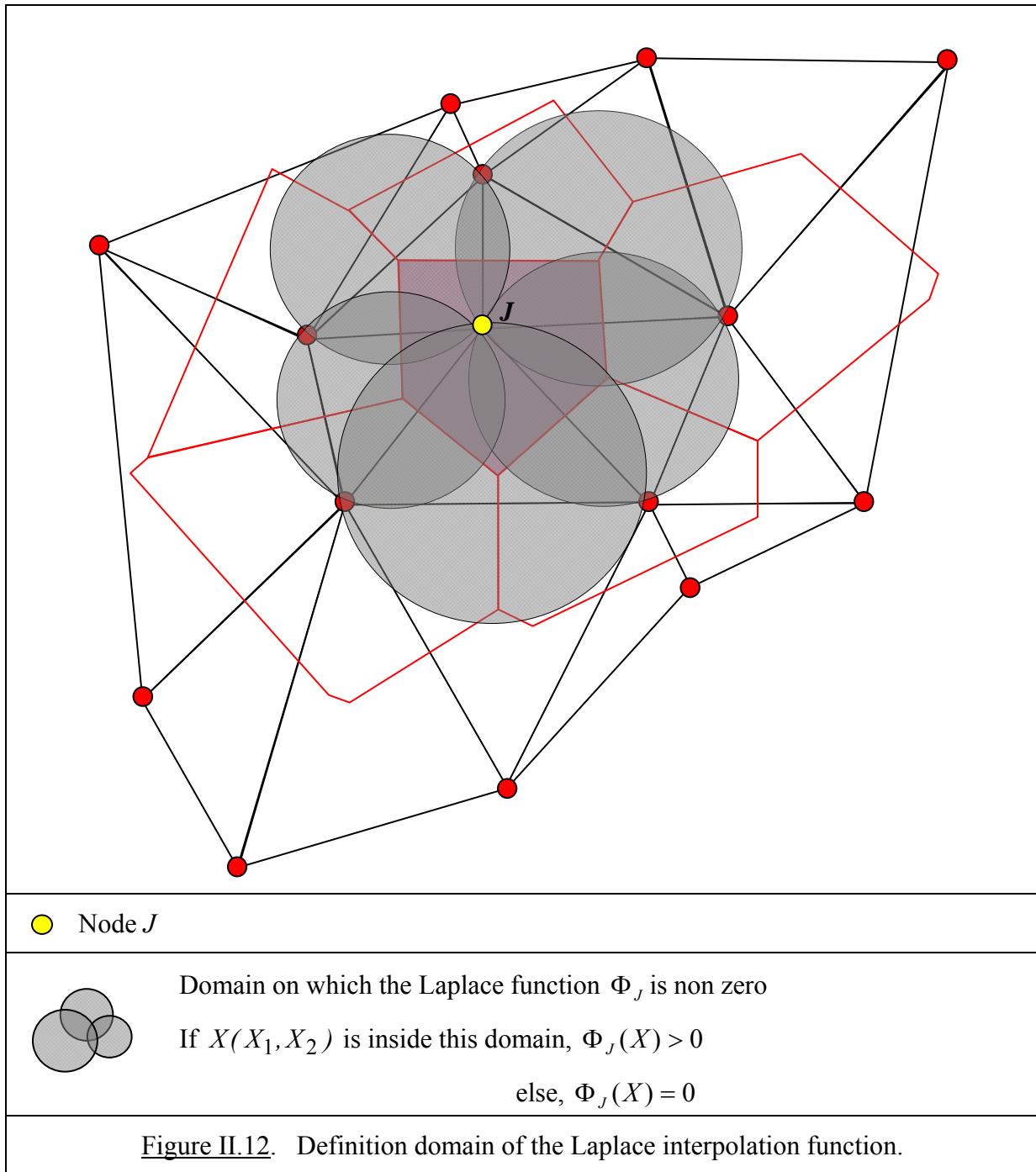
Bowyer-Watson algorithm: Step 1

Find the circumcircles inside which point $X(X_1, X_2)$ is located.

🔵 Point $X(X_1, X_2)$	
	The 3 circumcircles inside which point $X(X_1, X_2)$ is located

Figure II.13.a. Bowyer-Watson algorithm: step 1.
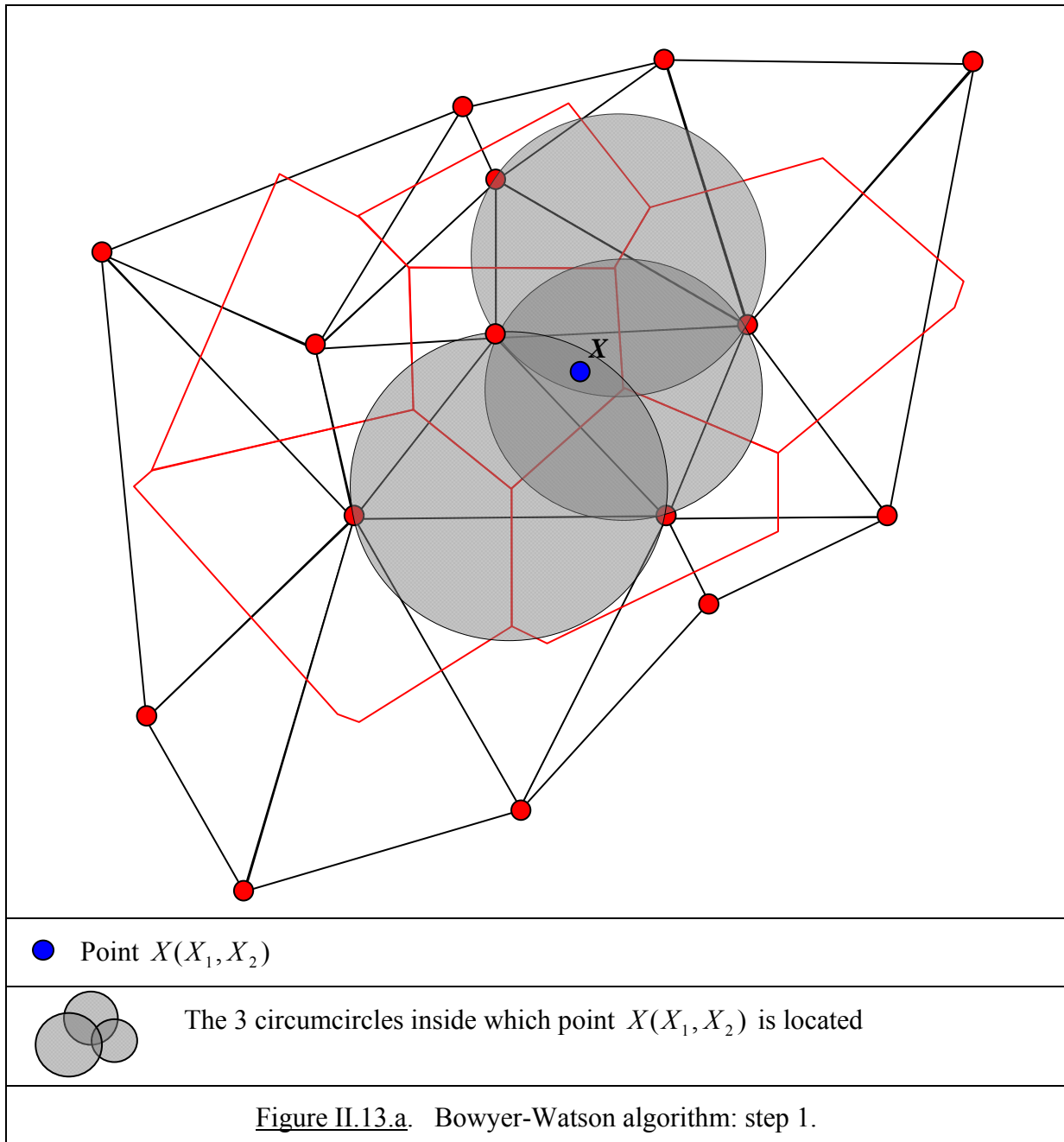
Bowyer-Watson algorithm: Step 2

Find the corresponding Delaunay triangles and delete the internal edges

🔵 Point $X(X_1, X_2)$		🟡 The natural neighbours of point $X(X_1, X_2)$

The 3 triangles corresponding to the 3 circumcircles found in step 1

<u>Figure II.13.b</u>.   Bowyer-Watson algorithm: step 2.
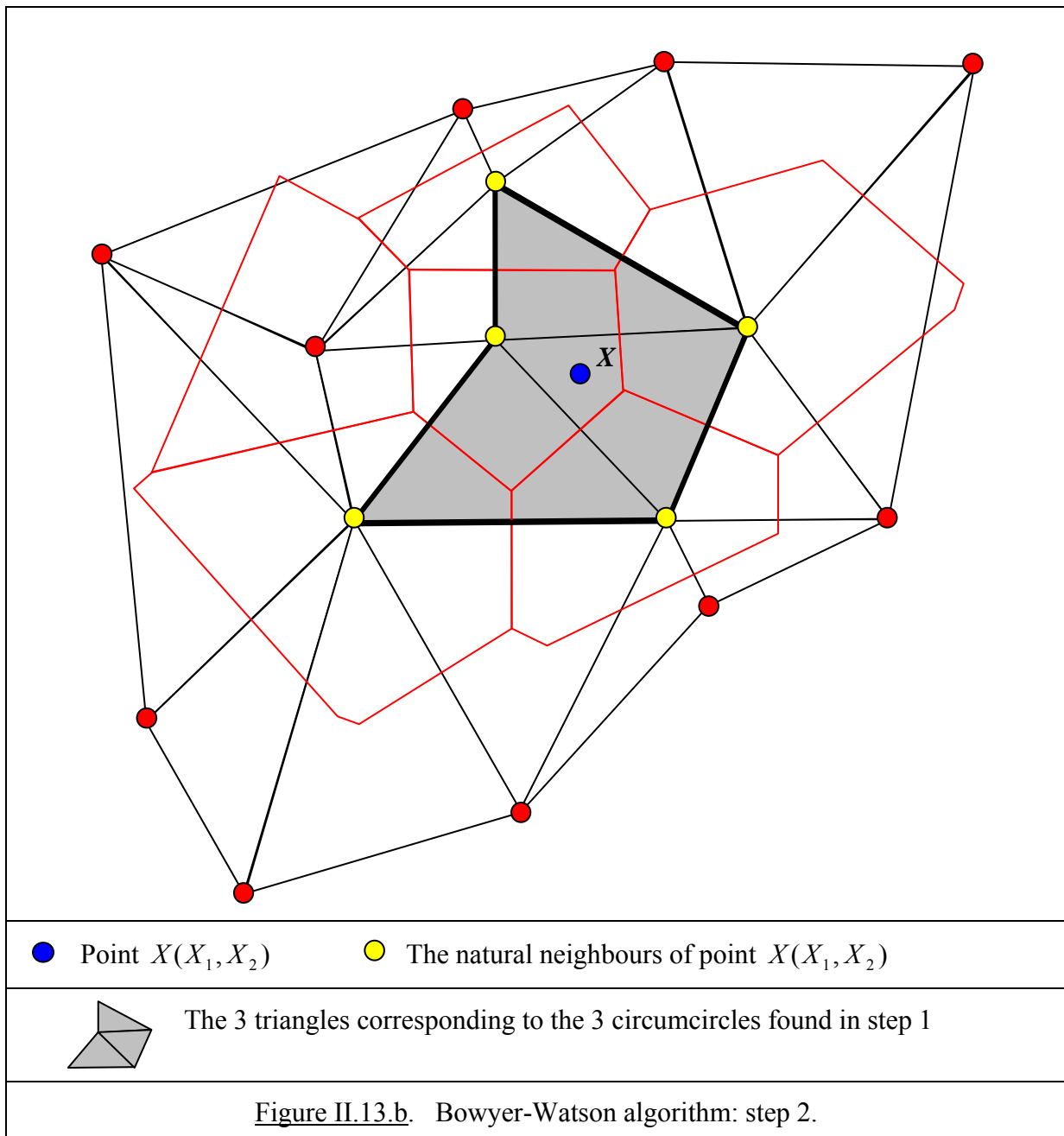
Bowyer-Watson algorithm: Step 3

In the set containing the initial nodes plus point $X(X_1, X_2)$, construct the Voronoi polygon associated with point $X(X_1, X_2)$.

●   Point $X(X_1, X_2)$ ○   The natural neighbours of point $X(X_1, X_2)$

The Voronoi polygon associated with point $X(X_1, X_2)$

Figure II.13.c.   Bowyer-Watson algorithm: step 3.
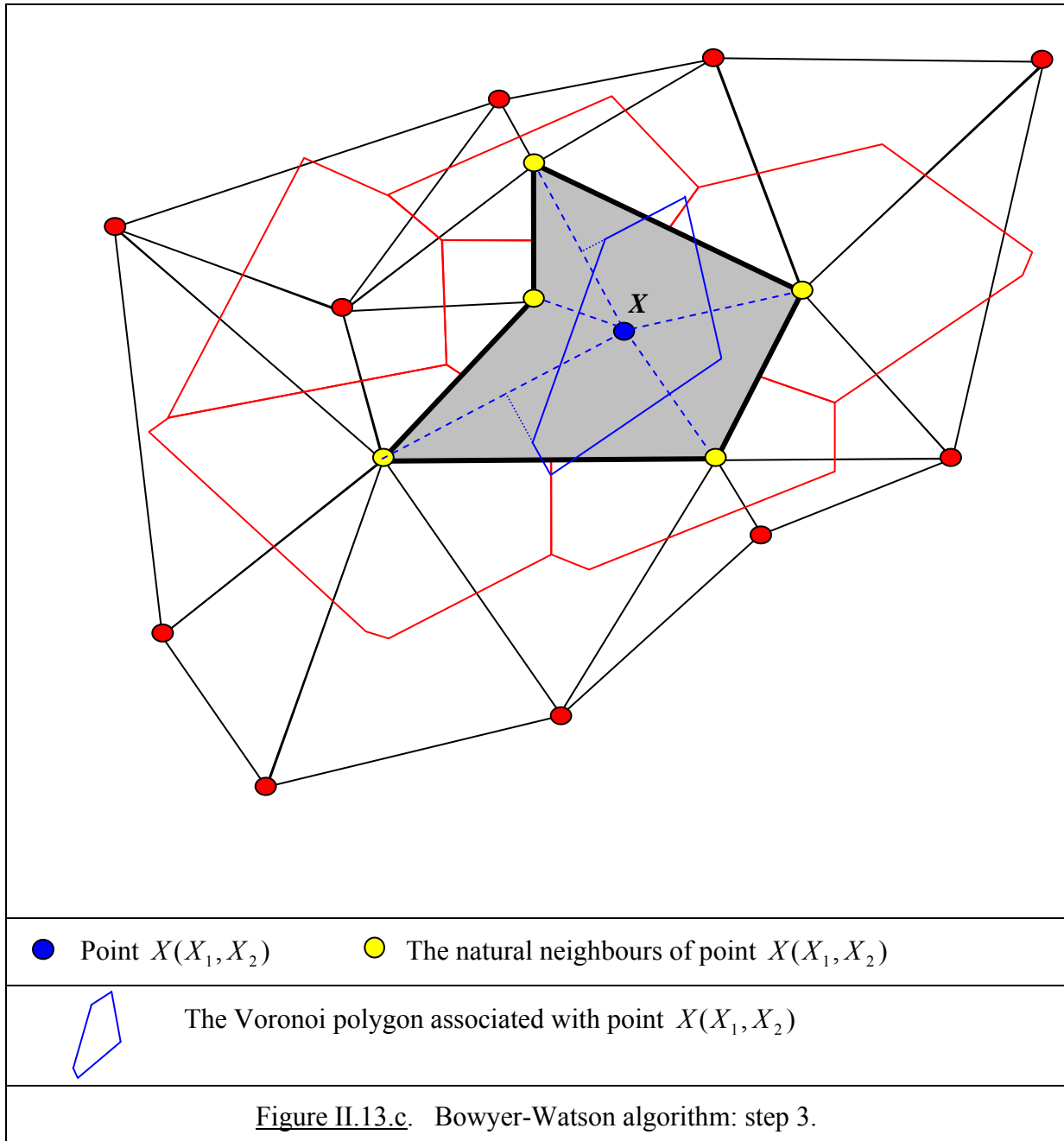
Bowyer-Watson algorithm: Step 4

Compute $\alpha_I(X) = \dfrac{s_I(X)}{h_I(X)}$ (II.4)

where h_I is the distance between point X and its natural neighbour I and s_I is the length of the edge of the Voronoi polygon perpendicular to X-I.

Then

$$\Phi_I(X) = \frac{\alpha_I(X)}{\sum \alpha_I(X)}$$ (II.5)

is the value of the Laplace interpolation function associated with node I computed at point X.

● Point $X(X_1, X_2)$ ○ The natural neighbours of point $X(X_1, X_2)$

The Voronoi polygon associated with point $X(X_1, X_2)$

<u>Figure II.13.d</u>. Bowyer-Watson algorithm: step 4.
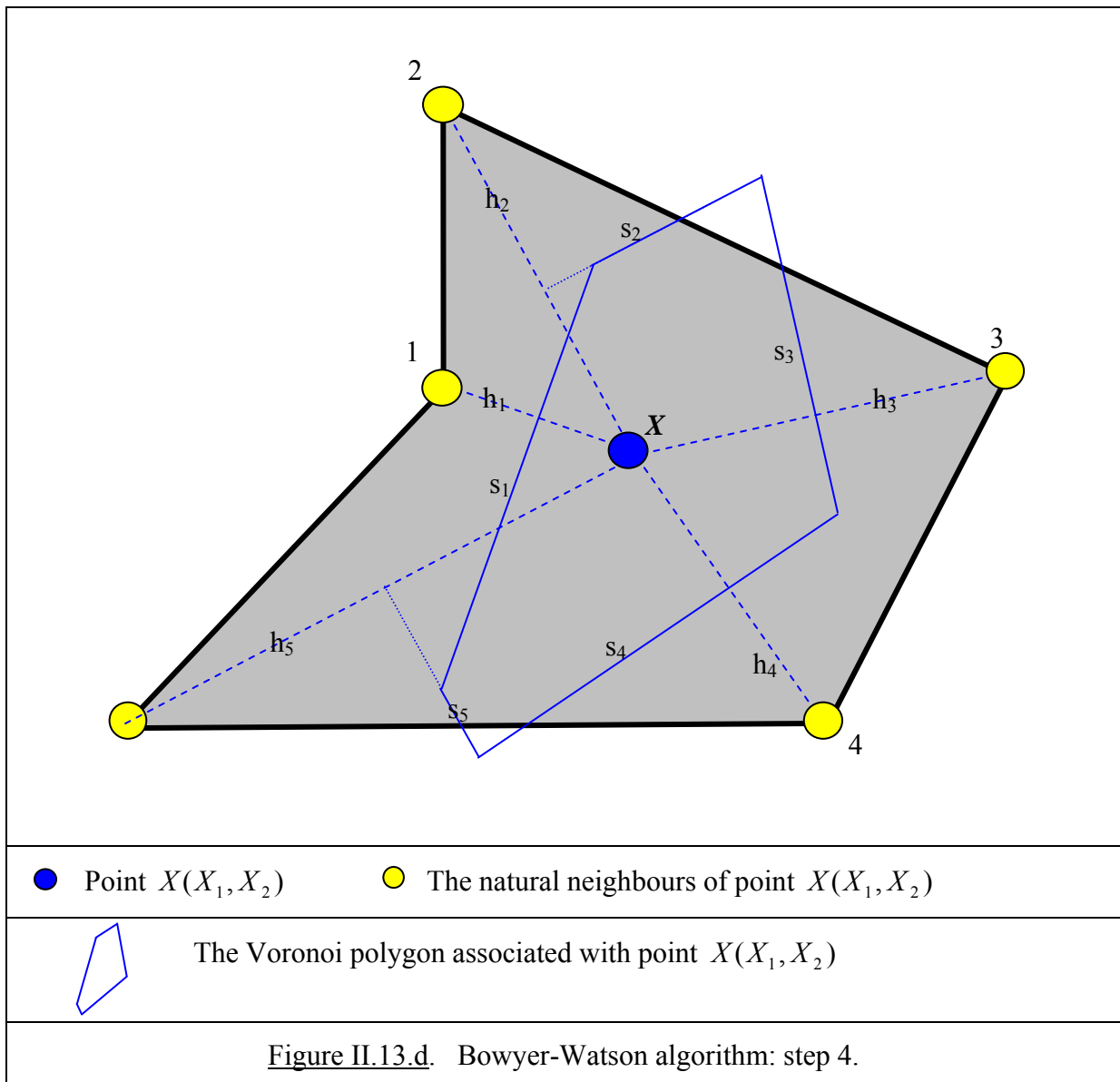
II.1.2.3. Laplace interpolation function for a point *X* on the domain contour

Consider point *X* belonging to the contour, for example between nodes 14 and 16 of figure II.14, such that its natural neighbours are nodes 14, 15, 16. The Voronoi polygon associated with *X* is indicated on figure II.14.

It is seen that $s_{14} = s_{16} = \infty$. From the definition of the Laplace interpolation function, it is easy to show [CUETO E. et al. (2003)] that:

$$\Phi_{14}(X) = 1 - \xi \qquad\qquad \Phi_{16}(X) = \xi \qquad\qquad \Phi_{K}(X) = 0 \ , \quad K \neq 14, 16$$

Figure II.14.   Laplace interpolation functions for point *X* ●
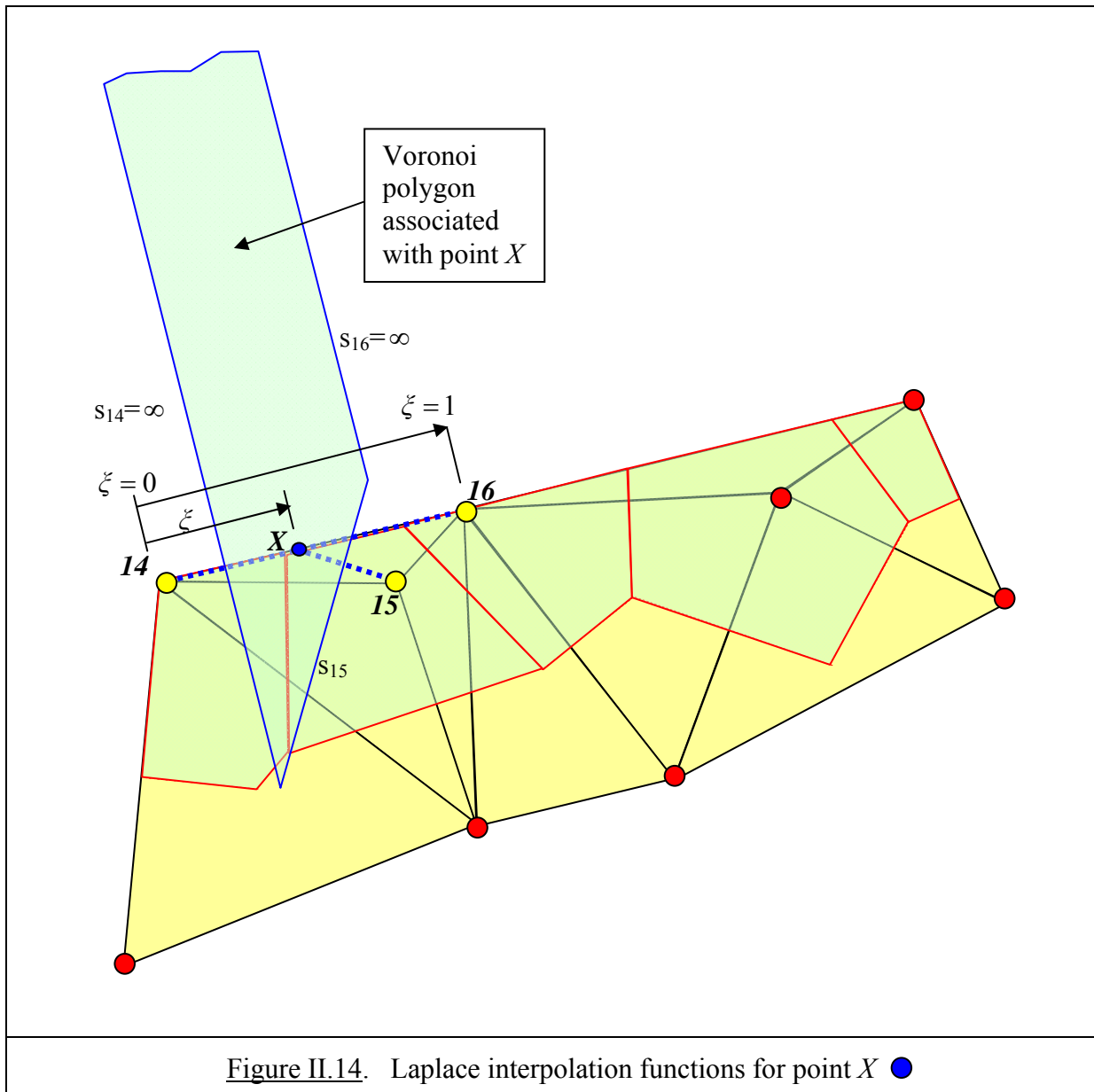
Consider now the case of figure II.15.

For the point X ● on a boundary near a non convex region, the natural neighbours can be the points ○ .

Points *6, 7, 26* are natural neighbours for any ξ .

Points *25, 27* are natural neighbours or not according to the value of ξ (for the particular position of X on the figure, they are not).

Note that, although the circumcircle of triangle *3-4-6* includes point X, points *3* and *4* are not natural neighbours of *X*.

Figure II.16 shows the Delaunay triangles in the vicinity of *X*. Point *X* has been added to the points of the domain to construct these triangles. The Voronoi polygons associated with this Delaunay triangulation are also shown.

It is seen that, for the chosen position of *X*, the polygon associated with *X* has common edges with the Voronoi polygons associated with points *6, 7, 26*. This simply means that, for the chosen position of *X*, its natural neighbours are points *6, 7, 26* .

It is also seen that the Voronoi polygon associated with *X* is unbounded.

Using the same arguments as above, it is easy to show that the Laplace interpolation functions are:

$$\Phi_{26}(X) = 1 - \xi$$

$$\Phi_6(X) = \xi$$

$$\Phi_K(X) = 0 , \quad K \neq 6, 26$$

So, even in the case of a non convex domain boundary, the Laplace interpolation functions for a point *X* on this boundary are linear functions of the position ξ of the point.

II.1.2.4. Properties of the Laplace interpolation function

It is easily verified that the Laplace interpolation functions have the following properties:

Kronecker delta property

$$0 \leq \Phi_J \leq 1, \quad \Phi_J(X_1^I, X_2^I) = \delta_{IJ} \tag{II.6}$$

Partition of unity property

$$\sum_{J=1}^{N} \Phi_J(X_1, X_2) = 1 \tag{II.7}$$

Linear completeness

$$\sum_{J=1}^{N} X_i^J \Phi_J(X_1, X_2) = X_i \tag{II.8}$$
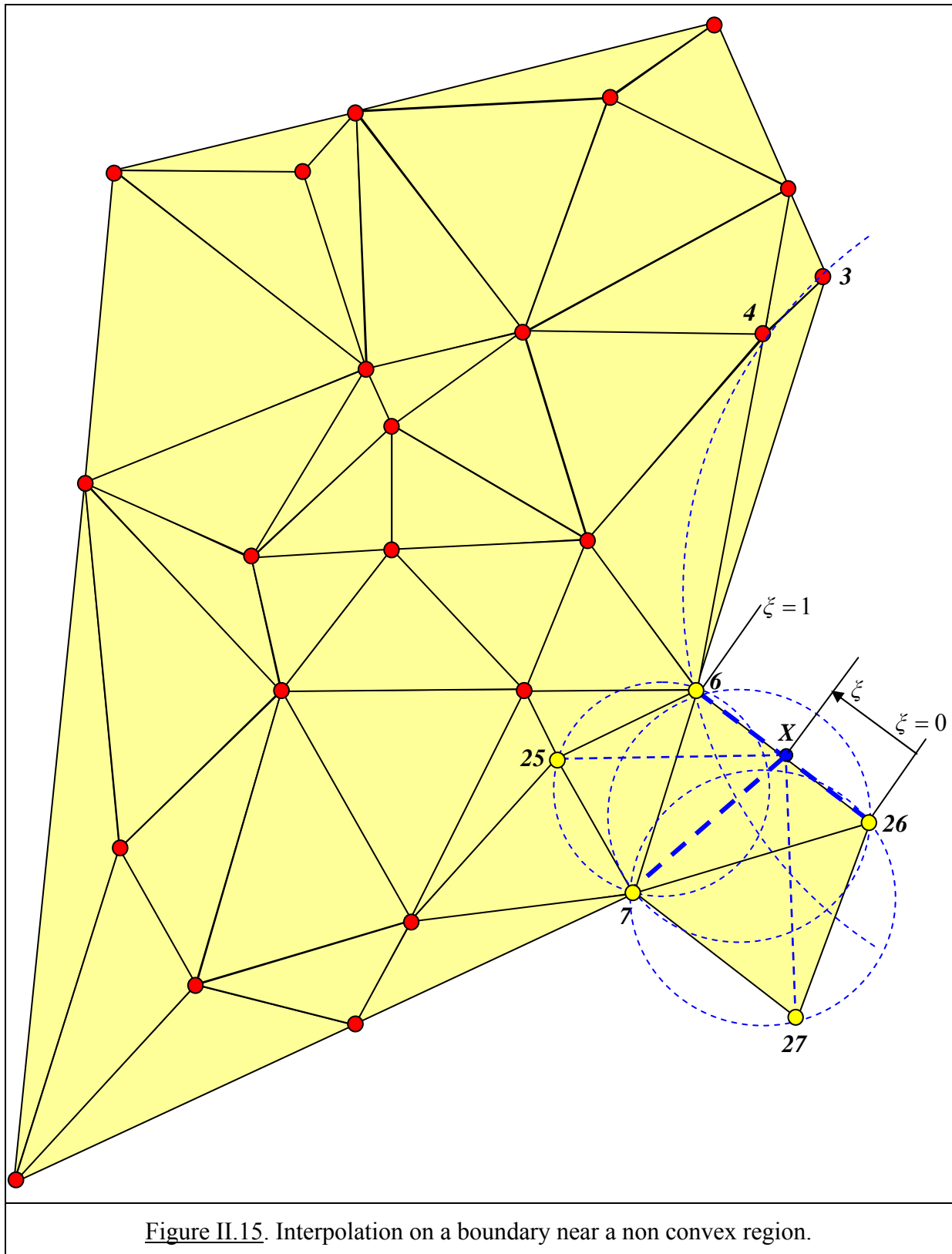
Figure II.15. Interpolation on a boundary near a non convex region.

Figure II.16. Interpolation on a boundary near a non convex region.

Text visible in figure:
6
25
X
26
27
7

Voronoi polygon Associated with point X
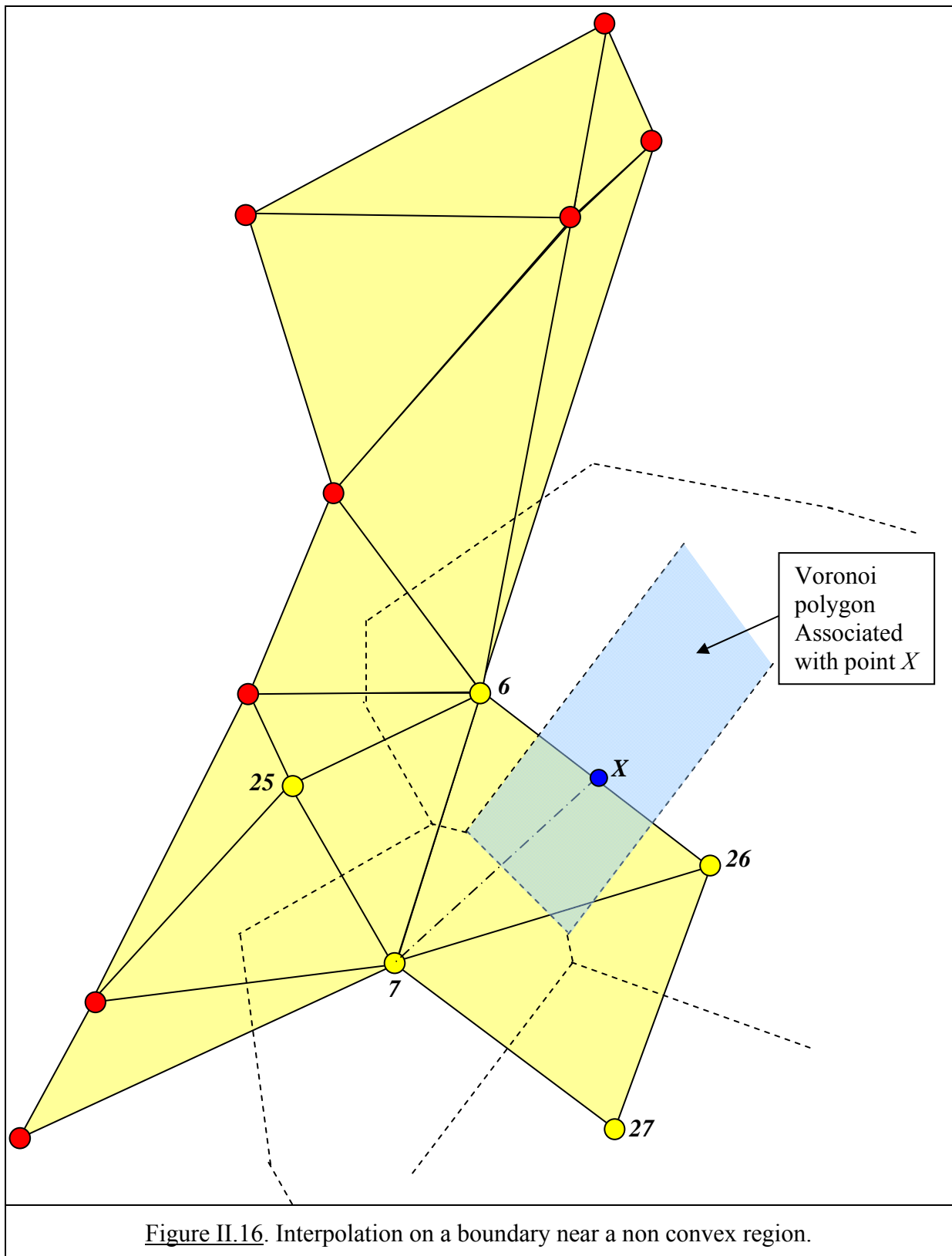
II.1.2.5. Example of Laplace function

For the domain of figure II.17, the Laplace function Φ_J associated with node J is illustrated at figure II.18 (from ILLOUL A. L. , 2008).
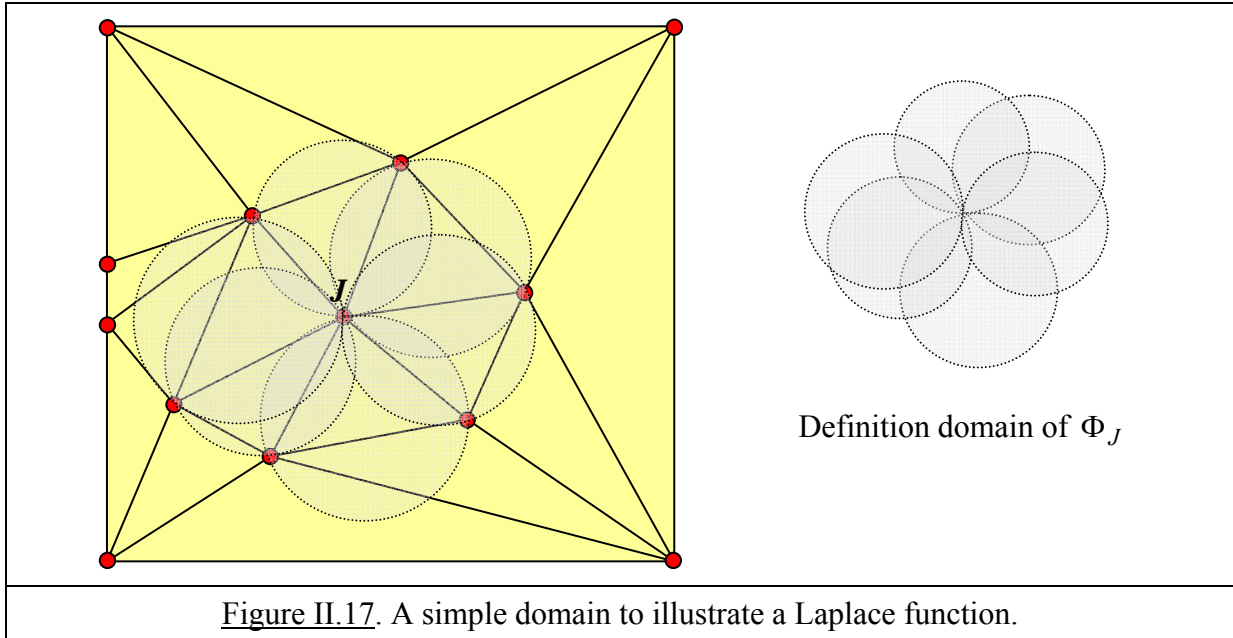

Definition domain of Φ_J

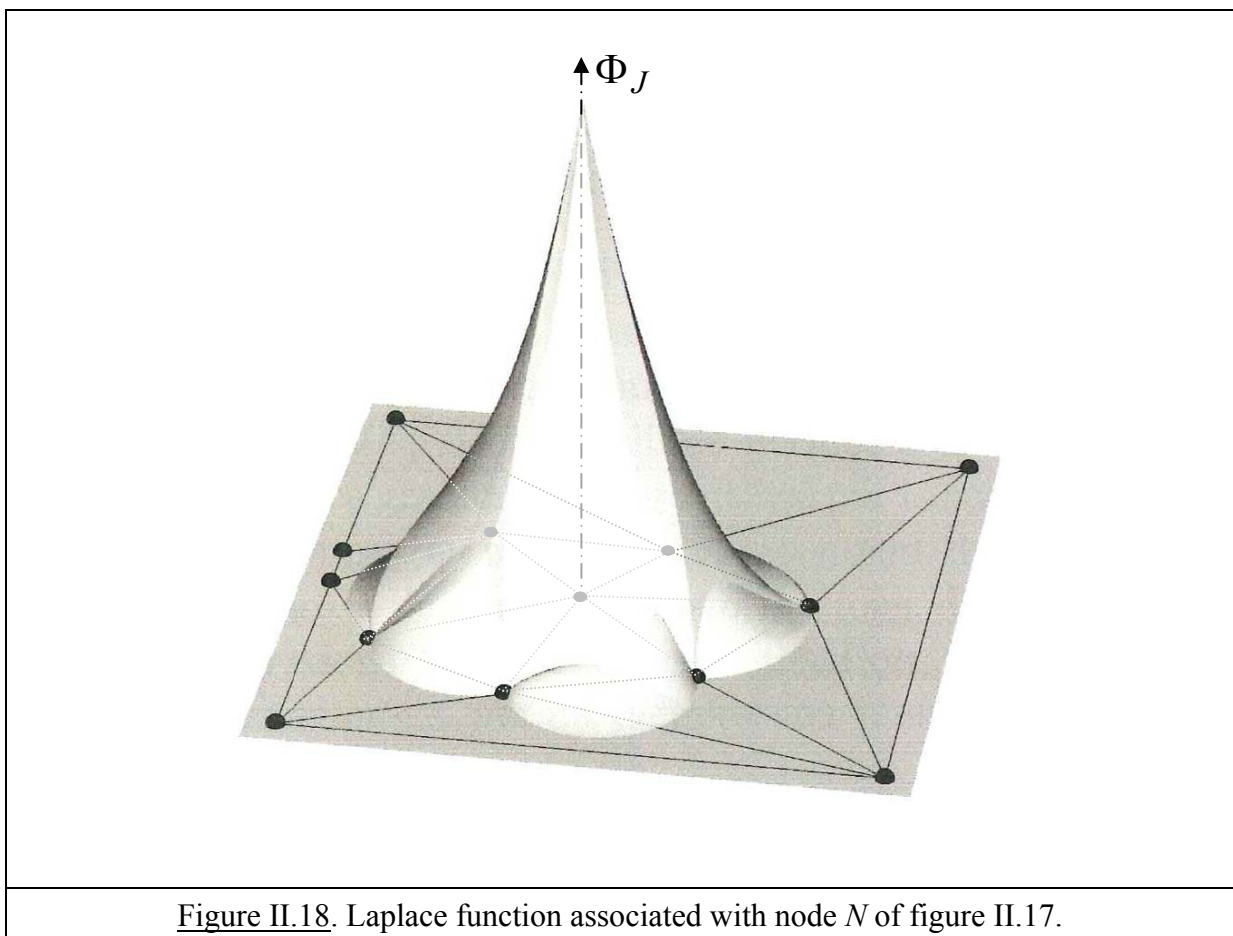Figure II.17. A simple domain to illustrate a Laplace function.

Φ_J

Figure II.18. Laplace function associated with node N of figure II.17.

II.2. The classical Natural Element Method

The natural neighbours method or natural element method (NEM) [SAMBRIDGE M. et al.(1996), SUKUMAR N. (1998), CUETO E. et al. (2003)] can be considered as one of the many variants of the meshless methods [NAYROLES B. et al. (1992), BELYTCHKO T. et al.(1996-a), LI K. and LIU W.K. (2002)].

Classically, the development of these methods is based on the virtual work principle.

A set of nodes are distributed over the domain to be studied and the displacement field is discretized with the help of interpolation functions that are not based on the finite element concept but only based on the nodes.

Typically, for a 2-dimensional elastic solid occupying the domain A, one has the following steps.

II.2.1. Virtual work principle

$$\int_A \sigma_{ij} \delta\varepsilon_{ij} \, dA - \int_A F_i \delta u_i \, dA - \int_{S_t} T_i \delta u_i \, dS = 0 \tag{II.9}$$

$$\delta\varepsilon_{ij} = \frac{1}{2}(\frac{\partial \delta u_i}{\partial X_j} + \frac{\partial \delta u_j}{\partial X_i}) \tag{II.10}$$

are the virtual strains associated with the virtual displacements δu_i

σ_{ij} are the Cauchy stresses deduced from the actual displacements u_i by Hooke's law:

$$\sigma_{ij} = C_{ijkl}\, \varepsilon_{kl} \tag{II.11}$$

with

$$\varepsilon_{kl} = \frac{1}{2}(\frac{\partial u_k}{\partial X_l} + \frac{\partial u_l}{\partial X_k}). \tag{II.12}$$

T_i are the surface tractions and F_i the body forces applied to the solid.

S_t is the part of the boundary where surface tractions are applied.

Usually, displacements $\widetilde{u}_i$ are imposed on the part S_u of the solid boundary.

II.2.2. Approximation of the displacement field

$$u_i = \sum_{J=1}^{N} \Phi_J u_i^J \tag{II.13}$$

$\Phi_J = \Phi_J(X_1, X_2)$ are the approximation functions

u_i^J are the nodal displacements

There are many different methods to choose this approximation.

Sometimes, it can be an interpolation as in the natural element method, i.e. the functions Φ_J satisfy the Kronecker delta property (II.6), the partition of unity property (II.7) and the linear completeness property (II.8).

But in some cases, as for the moving least square approximation [LANCASTER P. and SALKAUSKAS K. (1990)], the partition of unity property is not fulfilled so that the approximate nodal values are not equal to the exact nodal values:

$$u_i(X_1^K, X_2^K) = \sum_{J=1}^{N} \Phi_J(X_1^J, X_2^J) u_i^J \neq u_i^K \qquad \text{(II.14)}$$

II.2.3. Discretized virtual work principle

Introducing the discretized displacement field in the virtual work principle leads to the following classical development:

$$\sum_{J=1}^{N} \delta u_i^J \int_A \sigma_{ij} B_j^J dA - \sum_{J=1}^{N} \delta u_i^J P_i^J = 0 \quad \Rightarrow \quad \int_A \sigma_{ij} B_j^J dA = P_i^J \qquad \text{(II.15)}$$

$$P_i^J = \int_A F_i \Phi_J dA + \int_{S_t} T_i \Phi_J dS \qquad \text{(II.16)}$$

are the approximate (discretized) nodal loads;

B_j^J is the matrix relating the virtual strains to the virtual nodal displacements:

$$\delta\varepsilon_{ij} = \sum_{J=1}^{N} B_j^J \delta u_i^J \qquad \text{(II.17)}$$

This eventually leads to an equation system in which the nodal displacements are the unknowns.

With this approach, two points deserve special attention in meshless methods: the numerical evaluation of the integrals over the domain A [GONZALEZ D et al. (2004)] and the enforcement of boundary conditions of the type $u_i = \tilde{u}_i$ on S_u.

For the numerical integration, the most common practice is to use a "background mesh", that is to divide the domain A in sub-domains of simple shape (usually triangles and quadrangles) in which classical numerical quadrature rules can be applied. Usually, this requires a large number of integration points.

More sophisticated methods [ATLURI S.N. et al.(1999), ATLURI S.N. and ZHU T. (2000), CUETO E. et al. (2003)] take account of the shape of the support of the approximation function, i.e. of the area where this function is not equal to zero.

Generally, such methods do not give excellent results for the patch test [CUETO E. et al. (2003)].

On the other hand, a "stabilized conforming nodal integration for Galerkin meshfree methods" [CHEN J. S. et al. (2001), YOO J. et al. (2004)] has been proposed, the basic idea of which consists in averaging the strains ε_{kl} in the vicinity of a node I over the Voronoi cell A_I associated with this node:

$$\bar{\varepsilon}_{kl} = \frac{1}{A_I} \int_{A_I} \varepsilon_{kl} \, dA_I = \frac{1}{2A_I} \oint_{C_I} (N_k u_l + N_l u_k) dC_I \qquad \text{(II.18)}$$

where C_I is the contour of the Voronoi cell A_I and $N = (N_1, N_2)$ is the unit outward normal to C_I.

This idea has been successfully used [CUETO E. et al. (2003), YOO J. et al. (2004), YVONNET J. (2004), YVONNET J et al.(2004)]. Excellent results were obtained.

In particular, in [YVONNET J et al.(2004)], the stresses in the Voronoi cells are deduced from the averaged strains and the application of the divergence theorem allows avoiding numerical integration on the Voronoi cell and replaces it by an integral on its contour.

In [YAGAWA G. and MATSUBARA H. (2006)], an "enriched free mesh method" based on Heilinger-Reissner principle is proposed in which an hypothesis on the strains in a cluster of triangular finite elements surrounding a node is made. To some extend, this approach is also a kind of strain averaging procedure in the vicinity of a node.

For the enforcement of boundary conditions of the type $u_i = \widetilde{u}_i$ on S_u, there is a basic problem if the approximation functions Φ_J do not possess the linear completeness property. Indeed, in such a case, the approximated nodal displacements at a node K

$$u_i(X_1^K, X_2^K) = \sum_{J=1}^{N} \Phi_J(X_1^K, X_2^K) u_i^J \qquad \text{(II.19)}$$

cannot be equal to a displacement $\widetilde{u}_i^K$ imposed to this node.

Nevertheless, in [NAYROLES B. et al. (1992)], the condition $\sum_{J=1}^{N} \Phi_J(X_1^J, X_2^J) u_i^J = \widetilde{u}_i^K$ is imposed as an approximation.

Many different solutions have been proposed to remedy this difficulty: connexion with finite elements [KRONGAUZ Y. and BELYTCHKO T. (1996), BELYTCHKO T. et al.(1996)], modified variational principle with penalty [BELYTCHKO T. et al. (1994-b), GAVETTE L., et al. (2000)], modified variational principle with [BELYTCHKO T. et al. (1994-a)] or without [LU Y. et al.(1994)] Lagrange multipliers, introduction of singular weighting functions [KALJEVIC I. and SAIGAL S. (1997)], ...

On the other hand, the difficulty disappears if $\Phi(X_1, X_2)$ varies linearly when point $X = (X_1, X_2)$ moves between 2 neighbour nodes belonging to the contour.

We have seen in section II.1.2.2. above that it is the case when the Laplace interpolation function is adopted for $\Phi(X_1, X_2)$.

It is also the case if the Sibson interpolation function [SIBSON R. (1980)] is used.

II.2.4. Conclusion

The classical natural element method based on the virtual work principle is a powerful tool that has been developed initially in the domain of 2D linear elastic problems and subsequently extended to most domains of Solid Mechanics: non linear materials and large strains [YVONNET J. (2004), LORONG PH. et al. (2006), ILLOUL A. L. (2008)], 3D problems [ILLOUL A. L. (2008)], ...
Its main advantages are [CHINESTA F. et al, 2009]:
- the quality of interpolation is optimal for a given distribution of nodes: indeed, this interpolation, via the Delaunay triangles and the Voronoi cells, is based on the notion of natural neighbours, which means that the interpolation function associated with a given node takes account in the best possible way of the distribution of the other nodes in its vicinity;
- the interpolation functions become piecewise linear between the nodes of the domain contour, which provides the possibility to impose boundary conditions in the same way as with the finite element method;

The NEM can be extended to 3D problems.

In particular, in [ILLOUL A. L. (2008)], it is shown that for 3D linear elastic problems,

- this method gives better results than the finite element method (same quality of results with shorter computation time or results of better quality with same computation time);

- this method gives results of the same quality as the stabilized finite element method [LIU G. R. et al, 2007-a, 2007-b]

II.3. The Fraeijs de Veubeke (FdV) variational principle

II.3.1 Historical note

In his original paper of 1954 [HU H. C. (1954)], HU Hai Chang proposed the following functional for linear elasticity problems:

$$\Pi = \int_A L_U dA - \int_{S_u} N_j \Sigma_{ji} \widetilde{u}_i dS - \int_{S_t} u_i (N_j \Sigma_{ji} - T_i) dS \qquad (II.20)$$

with

$$L_U = \frac{\partial \Sigma_{ij}}{\partial X_j} u_i + F_i u_i + \varepsilon_{ij} \Sigma_{ij} - W(\varepsilon_{ij}) \qquad (II.21)$$

with A the area of the domain (i.e. the 2D solid), S the contour of the domain, N_j the outward normal to this contour, S_t and S_u the parts of S on which surface tractions T_i and displacements $\widetilde{u}_i$ are respectively imposed.

This functional has 3 fields:

$\Pi = \Pi(u_i, \Sigma_{ij}, \varepsilon_{ij})$

u_i : the displacement field

Σ_{ij} : the stress field

ε_{ij} : the strain field

The variable $W(\varepsilon_{ij})$ is the energy density function from which "constitutive stresses" can be deduced by

$$\sigma_{ij} = \frac{\partial W}{\partial \varepsilon_{ij}} \qquad (II.22)$$

It is easy to show that (II.20) is equivalent to:

$$\Pi = \int_A W(\varepsilon_{ij}) dA + \int_A \Sigma_{ij} \left[\frac{1}{2} \left(\frac{\partial u_i}{\partial X_j} + \frac{\partial u_j}{\partial X_i} \right) - \varepsilon_{ij} \right] dA - \int_A F_i u_i dA - \int_{S_t} T_i u_i dS + \int_{S_u} N_j \Sigma_{ji} (\widetilde{u}_i - u_i) dS$$

$$(II.23)$$

In 1955, this functional was also proposed independently by [WASHIZU K. (1955)].

It is generally known as the HU-WASHIZU functional.

However, an article published in 2000 [FELIPPA C. A. (2000)] shows that a more general functional had been proposed as early as 1951 by FRAEIJS de VEUBEKE [FRAEIJS de VEUBEKE B. M. (1951)].

This functional can be written as follows.

$\Pi(u_i, \varepsilon_{ij}, \Sigma_{ij}, r_i) =$

$$\int_A W(\varepsilon_{ij})dA + \int_A \Sigma_{ij}\left[\frac{1}{2}(\frac{\partial u_i}{\partial X_j} + \frac{\partial u_j}{\partial X_i}) - \varepsilon_{ij}\right]dA - \int_A F_i u_i dA - \int_{S_t} T_i u_i dS + \int_{S_u} r_i(\widetilde{u}_i - u_i)dS$$

(II.24)

It has an additional independent field r_i that can be identified as assumed surface support reactions on S_u.

It is this functional that will be used in the present thesis as the starting point of an original approach of the natural elements method.

If it is assumed a priori that the surface support reactions on S_u are in equilibrium with the assumed stresses Σ_{ij}, the HU-WASHIZU functional is recovered as a particular case of the FRAEIJS de VEUBEKE functional.

II.3.2. The Fraeijs de Veubeke variational principle

The variation of $\Pi = \Pi(u_i, \Sigma_{ij}, \varepsilon_{ij}, r_i)$ can be written as follows:

$$\delta\Pi_1 = \int_A \delta W(\varepsilon_{ij})dA = \int_A \sigma_{ij}\delta\varepsilon_{ij}dA$$

(II.25)

$$\delta\Pi_2 = \int_A \Sigma_{ij}\left[\frac{1}{2}(\frac{\partial\delta u_i}{\partial X_j} + \frac{\partial\delta u_j}{\partial X_i}) - \delta\varepsilon_{ij}\right]dA$$

(II.26)

$$\delta\Pi_3 = \int_A \delta\Sigma_{ij}\left[\frac{1}{2}(\frac{\partial u_i}{\partial X_j} + \frac{\partial u_j}{\partial X_i}) - \varepsilon_{ij}\right]dA$$

(II.27)

$$\delta\Pi_4 = -\int_A F_i \delta u_i dA$$

(II.28)

$$\delta\Pi_5 = -\int_{S_t} T_i \delta u_i dS$$

(II.29)

$$\delta\Pi_6 = \int_{S_u} \delta r_i(\widetilde{u}_i - u_i)dS - \int_{S_u} r_i \delta u_i dS$$

(II.30)

The FdV variational principle simply postulates that the stresses, strains, displacements and support reactions that actually appear in the solid (loaded by the surface tractions T_i, the body forces F_i and submitted to the imposed displacements $\widetilde{u}_i$) make the FdV functional stationary.

Hence, these stresses, strains, displacements and support reactions are the solution of the equation:

$$\delta\Pi = \delta\Pi_1 + \delta\Pi_2 + \delta\Pi_3 + \delta\Pi_4 + \delta\Pi_5 + \delta\Pi_6 = 0$$

(II.31)

The first term of (II.26) can be integrated by parts:

$$\int_A \Sigma_{ij} \left[\frac{1}{2}(\frac{\partial \delta u_i}{\partial X_j} + \frac{\partial \delta u_j}{\partial X_i}) \right] dA = \oint_S N_j \Sigma_{ji} \delta u_i \, dS - \int_A \frac{\partial \Sigma_{ji}}{\partial X_j} \delta u_i \, dA \tag{II.32}$$

with

$$\int_S N_j \Sigma_{ji} \delta u_i \, dS = \int_{S_u} N_j \Sigma_{ji} \delta u_i \, dS + \int_{S_t} N_j \Sigma_{ji} \delta u_i \, dS \tag{II.33}$$

For the linear elastic case, the following classical equations are used:

$$\sigma_{ij} = \frac{\partial W(\varepsilon_{ij})}{\partial \varepsilon_{ij}} \tag{II.34}$$

and

$$W(\varepsilon_{ij}) = \frac{1}{2} C_{ijkl} \, \varepsilon_{ij} \, \varepsilon_{kl} \tag{II.35}$$

where C_{ijkl} is the classical Hooke's tensor.

Introducing these results in (II.31), we get:

$$\delta \Pi = \int_A (\sigma_{ij} - \Sigma_{ij}) \delta \varepsilon_{ij} \, dA - \int_A (\frac{\partial \Sigma_{ji}}{\partial X_j} + F_i) \delta u_i \, dA + \int_A \delta \Sigma_{ij} \left[\frac{1}{2}(\frac{\partial u_i}{\partial X_j} + \frac{\partial u_j}{\partial X_i}) - \varepsilon_{ij} \right] dA$$

$$+ \int_{S_u} (N_j \Sigma_{ji} - r_i) \delta u_i \, dS + \int_{S_t} (N_j \Sigma_{ji} - T_i) \delta u_i \, dS + \int_{S_u} \delta r_i (\tilde{u}_i - u_i) \, dS = 0 \tag{II.36}$$

which constitutes the FdV variational principle.

The corresponding Euler equations are summarized in table II.1.

Table II.1. Euler equations of the FdV variational principle		
Variation	Equation	Comments
$\delta \varepsilon_{ij}$ in A	$\sigma_{ij} = \Sigma_{ij}$	The assumed stresses are identified as the constitutive stresses inside the domain
$\delta \Sigma_{ij}$ in A	$\frac{1}{2}(\frac{\partial u_i}{\partial X_j} + \frac{\partial u_j}{\partial X_i}) = \varepsilon_{ij}$	Compatibility between the assumed strains and the assumed displacements inside the domain
δr_i on S_u	$u_i = \tilde{u}_i$	Compatibility between the assumed displacements and the displacements imposed on the part S_u of the domain contour
δu_i in A	$\frac{\partial \Sigma_{ji}}{\partial X_j} + F_i = 0$	Equilibrium inside the domain between the assumed stresses and the body forces
δu_i on S_t	$N_j \Sigma_{ji} = T_i$	Equilibrium on the part S_t of the domain contour where surface tractions are imposed
δu_i on S_u	$N_j \Sigma_{ji} = r_i$	Equilibrium on the part S_u of the domain contour where displacements are imposed

This table shows that all the pertinent equations of linear elastic Solid Mechanics are recovered as the solution of (II.31).

Obviously, this validates the FdV variational principle.

II.4. Linear Elastic Fracture mechanics (LEFM)

II.4.1. Introduction

The elements of fracture mechanics recalled hereafter are classical and can be found in any textbook on fracture mechanics.

The goal of this section is just to present the notions and formulae that will be used in chapters V and VI of this thesis to make their redaction simpler and allow the reader to concentrate on the original approaches developed in those chapters.

The presentation is limited to the 2D case for brittle materials that are elastic up to fracture.

II.4.2. Total potential energy

The notions of energy play an important role in LEFM. The following ones are used:

Potential energy of the applied forces:
$$V = -\int_A F_i u_i \, dA - \int_{S_t} T_i u_i \, dS \tag{II.37}$$

Strain energy:
$$W = \int_A \frac{1}{2} \sigma_{ij} \varepsilon_{ij} \, dA \tag{II.38}$$

Total potential energy:
$$\Pi = W + V = \int_A \frac{1}{2} \sigma_{ij} \varepsilon_{ij} \, dA - \int_A F_i u_i \, dA - \int_{S_t} T_i u_i \, dS \tag{II.39}$$
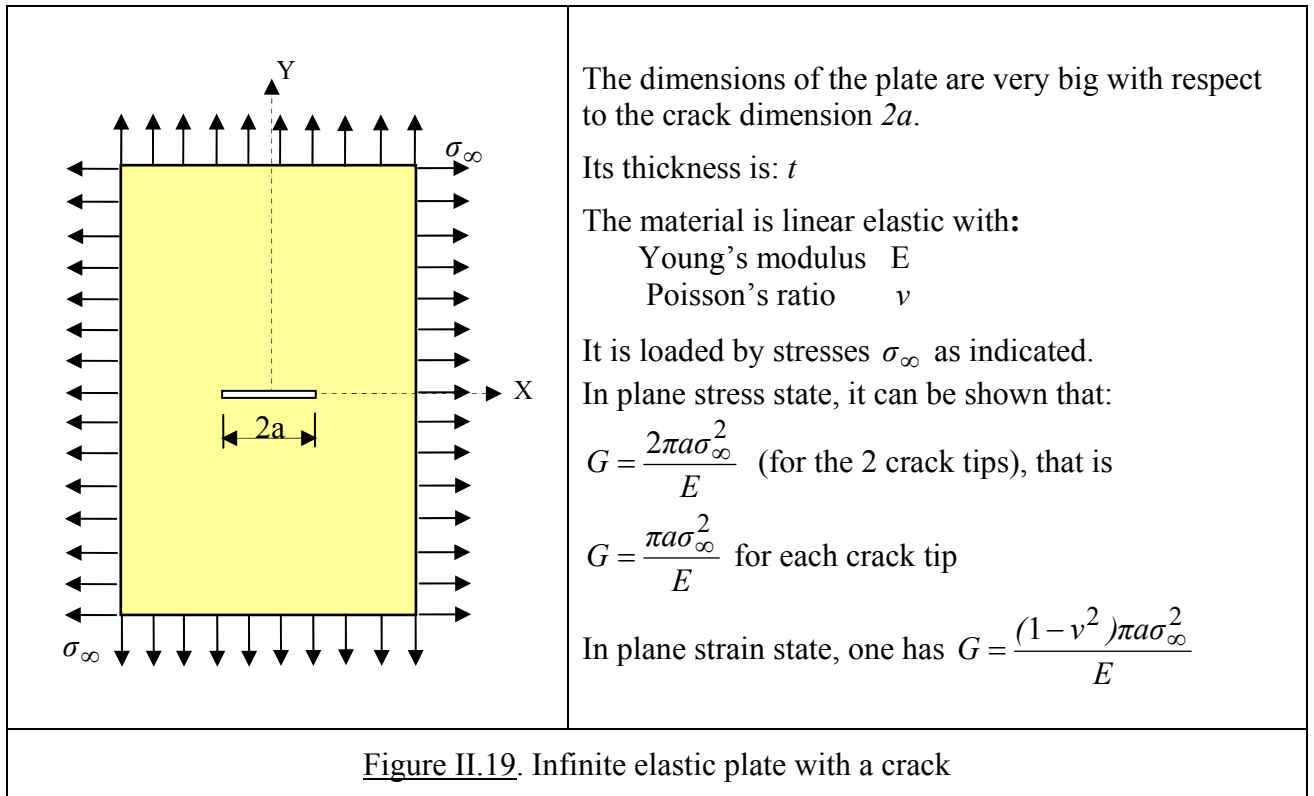
II.4.3. Energy release rate

In a solid in which a crack is present, the energy release rate G is defined by

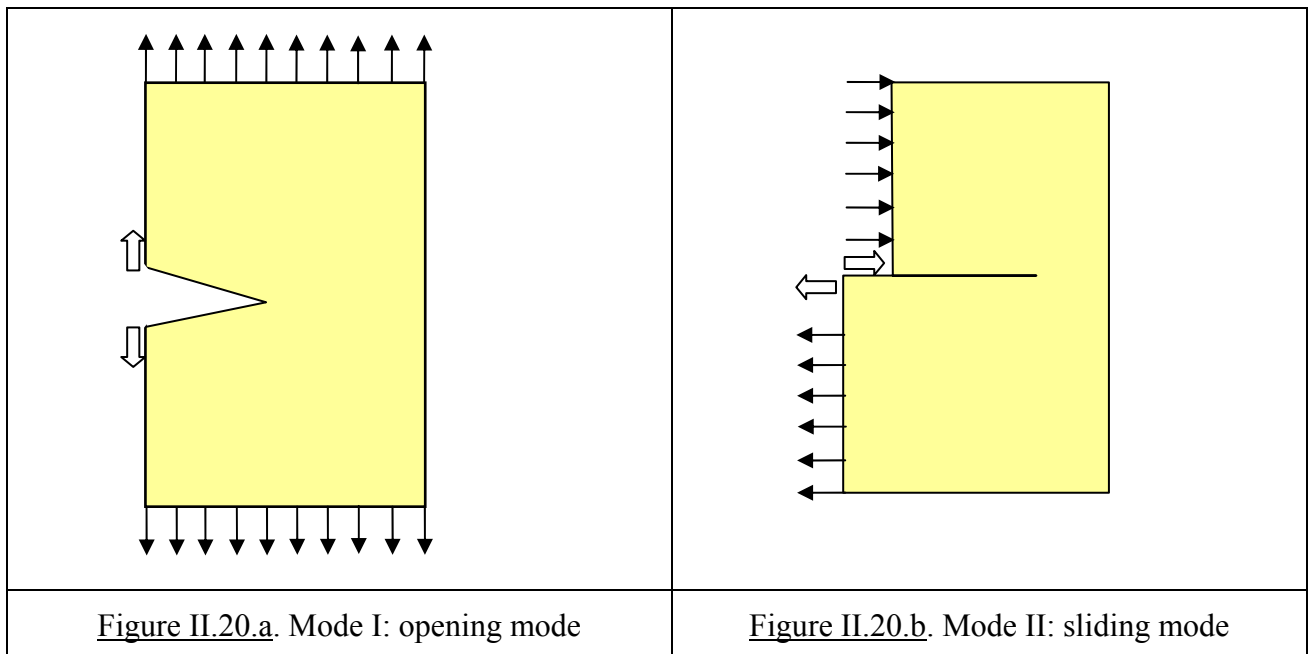$$G = -\frac{d\Pi}{dA_c} \tag{II.40}$$

where A_c is the cracked area. It is an expression of the decrease of the potential energy when the area of the crack increases.

The example of figure II.19 shows that G is a function of the crack area, of the loading and of the elastic properties of the material.

The dimensions of the plate are very big with respect to the crack dimension *2a*.

Its thickness is: *t*

The material is linear elastic with**:**
    Young's modulus   E
     Poisson's ratio   *v*

It is loaded by stresses σ_∞ as indicated.
In plane stress state, it can be shown that:

$$G = \frac{2\pi a \sigma_\infty^2}{E} \quad \text{(for the 2 crack tips), that is}$$

$$G = \frac{\pi a \sigma_\infty^2}{E} \quad \text{for each crack tip}$$

In plane strain state, one has $G = \dfrac{(1-v^2)\pi a \sigma_\infty^2}{E}$

Figure II.19. Infinite elastic plate with a crack

II.4.4. Fracture modes

In 2D, there are 2 main fracture modes shown in figure II.20.

Figure II.20.a. Mode I: opening mode

Figure II.20.b. Mode II: sliding mode

II.4.5. Stress intensity factors

The stress distribution near the crack tip can be expressed in a local reference system (r, θ) shown on figure II.21.

Figure II.21.a. Mode I: crack tip coordinates	Figure II.21.b. Mode II: crack tip coordinates
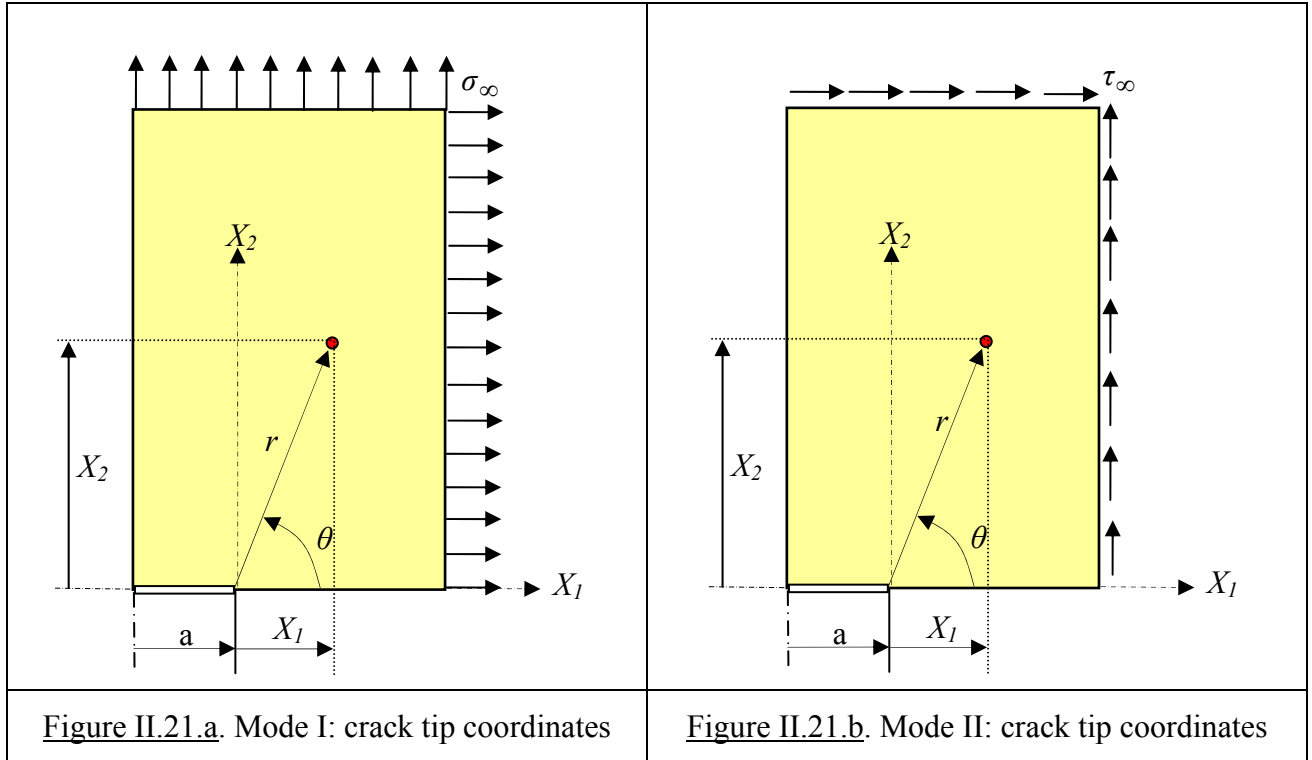
We consider a crack of length *2a* (on figure II.21, only a quarter of the domain is represented) submitted either to mode I loading or to mode II loading.

The stress fields near the crack ($r <<< $) tip are approximately given by [WESTERGAARD, H.M. (1939)]:

for mode I:
$$\begin{Bmatrix} \sigma_{11} \\ \sigma_{22} \\ \sigma_{12} \end{Bmatrix} = \frac{K_I}{\sqrt{2\pi r}} \cos\frac{\theta}{2} \begin{Bmatrix} 1 - \sin\frac{\theta}{2}\ \sin\frac{3\theta}{2} \\ 1 + \sin\frac{\theta}{2}\ \sin\frac{3\theta}{2} \\ \sin\frac{\theta}{2}\ \cos\frac{3\theta}{2} \end{Bmatrix} \qquad (II.41)$$

for mode II:
$$\begin{Bmatrix} \sigma_{11} \\ \sigma_{22} \\ \sigma_{12} \end{Bmatrix} = \frac{K_{II}}{\sqrt{2\pi r}} \begin{Bmatrix} -\sin\frac{\theta}{2}(2 + \cos\frac{\theta}{2}\ \cos\frac{3\theta}{2}) \\ \cos\frac{\theta}{2}\sin\frac{\theta}{2}\ \cos\frac{3\theta}{2} \\ \cos\frac{\theta}{2}(1 - \sin\frac{\theta}{2}\ \sin\frac{3\theta}{2}) \end{Bmatrix} \qquad (II.42)$$

These stresses are valid for both plane stress and plane strain conditions.

The displacement fields near the crack tip are given by:

for mode I:

$$\begin{Bmatrix} u_1 \\ u_2 \end{Bmatrix} = \frac{K_I}{2\mu} \sqrt{\frac{r}{2\pi}} \begin{Bmatrix} \left[\kappa - 1 + 2(\sin\frac{\theta}{2})^2 \right] \cos\frac{\theta}{2} \\ \left[\kappa + 1 - 2(\cos\frac{\theta}{2})^2 \right] \sin\frac{\theta}{2} \end{Bmatrix}$$

(II.43)

for mode II:

$$\begin{Bmatrix} u_1 \\ u_2 \end{Bmatrix} = \frac{K_{II}}{2\mu} \sqrt{\frac{r}{2\pi}} \begin{Bmatrix} \left[\kappa + 1 + 2(\cos\frac{\theta}{2})^2 \right] \sin\frac{\theta}{2} \\ \left[-\kappa + 1 + 2(\sin\frac{\theta}{2})^2 \right] \cos\frac{\theta}{2} \end{Bmatrix}$$

(II.44)

with

$$\mu = \frac{E}{2(1+v)} \text{ (shear modulus)},$$

(II.45)

$$\kappa = \begin{cases} 3 - 4v & \text{in plane strain state} \\ \dfrac{3-v}{1+v} & \text{in plane stress state} \end{cases}$$

(II.46)

K_I and K_{II} are the stress intensity factors of modes I and II respectively. They are given by:

$$K_I = \sigma_\infty \sqrt{\pi a}$$

(II.47)

$$K_{II} = \tau_\infty \sqrt{\pi a}$$

(II.48)

So, the general expression of stresses near the crack tip is:

$$\sigma_{ij} = \frac{K}{\sqrt{2\pi r}} f_{ij}(\theta) \text{ for } r <<<$$

(II.49)

It is also possible to calculate the energy release rate for the 2 modes.

The results are:

for mode I:

$$G = \frac{K_I^2}{E^*}$$

(II.50)

for mode II:

$$G = \frac{K_{II}^2}{E^*}$$

(II.51)

with

$$E^* = \begin{cases} \dfrac{E}{1-v^2} & \text{in plane strain state} \\ \\ E & \text{in plane stress state} \end{cases}$$

(II.52)

These results are based on the hypothesis that the crack grows in its own direction.

II.4.6. The *J* integral

Let Ω be a domain enclosed in a contour Γ around the crack tip as indicated on figure II.22.
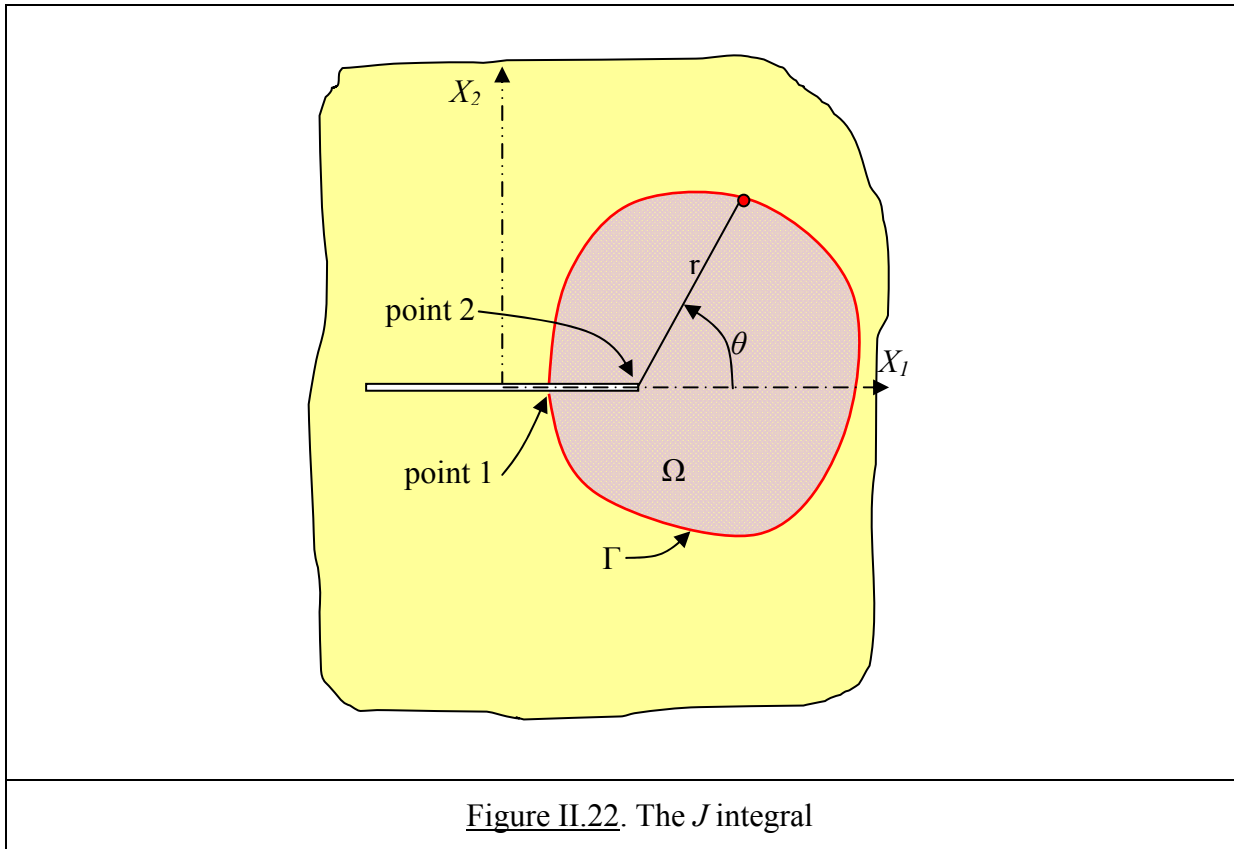

Figure II.22. The *J* integral

The total potential energy corresponding to this domain is:

$$\Pi_\Omega = W_\Omega + V_\Omega = \int_\Omega \frac{1}{2}\sigma_{ij}\varepsilon_{ij}\,dA - \int_\Omega F_i u_i\,dA - \int_{\Omega_t} T_i u_i\,dS \tag{II.53}$$

It can be shown that

$$G_\Omega = -\frac{d\Pi_\Omega}{da} = J_\Omega = \int_\Gamma (U_0\delta_{1j} - \sigma_{ij}\frac{\partial u_i}{\partial x_1})N_j\,d\Gamma \tag{II.54}$$

G_Ω is the release rate of the potential energy Π_Ω.

If:

- the lips of the crack are not loaded
- the crack is straight between points 1 (beginning and end of Γ) and 2 (crack tip)

then, it can be proven that J_Ω is independent of the chosen contour Γ.

Consequently, we may write:

$$G = -\frac{d\Pi}{da} = J = \int_\Gamma (U_0\delta_{1j} - \sigma_{ij}\frac{\partial u_i}{\partial x_1})N_j\,d\Gamma \tag{II.55}$$

So, the *J* integral can be used to calculate the energy release rate and, subsequently, the stress intensity factors.

II.5. Conclusion

The 2 basic tools presented above, i.e. the Natural Element Method (NEM) and the FRAEIJS de VEUBEKE (FdV) variational principle will appear in each subsequent chapter of the present thesis.

The starting point of the thesis is the observation that the FdV variational principle, with its 4 independent fields $u_i, \Sigma_{ij}, \varepsilon_{ij}, r_i$, offers a lot of flexibility to choose discretization hypotheses on these fields for the numerical solution of Solid Mechanics problems..

Hence, an original approach of the NEM will be developed on the basis of the FdV variational principle instead of the virtual work principle.

This approach will be first explored for linear elastic problems (chapter III).

Then, it will be extended to materially non linear problems (chapter IV) and to linear fracture mechanics problems (chapter V).

Finally, in chapter VI, by analogy with the eXtended Finite Element Method (XFEM), an eXtended Natural Element Method (XNEM) will be proposed for linear fracture mechanics.